

Supporting Information

to

Synthesis and Characterization of Long chain *O*-acyl-L-alaninols and Investigation of Drug Encapsulation and Release by Equimolar *O*-Myristoyl-L-Alaninol/SDS Catanionic Liposomes

Suman Kumar Choudhury, Ravindar Chinapaka, Konga Manasa, Musti J. Swamy*

School of Chemistry, University of Hyderabad, Hyderabad-500 046, India

Running title: Characterization of *O*-acyl-L-alaninols and their catanionic liposomes with SDS

*Corresponding author:

Prof. Musti J. Swamy, School of Chemistry, University of Hyderabad, Hyderabad - 500 046, India. Tel: +91-40-2313-4807, E-mail: mjswamy@uohyd.ac.in, mjswamy1@gmail.com

Materials and Methods

Analysis of ITC data by one set of sites binding model

For a system of one set of identical binding sites, the total heat evolved or absorbed during the binding process at the end of the i^{th} injection, $Q(i)$, is given by Eq. 1:

$$Q(i) = \frac{n P_t \Delta H V \left\{ 1 + \frac{X_t}{n P_t} + \frac{1}{n K P_t} - \left[\left(1 + \frac{X_t}{n P_t} + \frac{1}{n K P_t} \right)^2 - \frac{4 X_t}{n P_t} \right]^{\frac{1}{2}} \right\}}{2} \quad (1)$$

Where

$Q(i)$: total heat evolved (or absorbed) during the binding process at the end of the i^{th} injection

n : total number of binding sites present on the protein

P_t : total protein concentration

X_t : total ligand concentration

V : volume of the cell

K : binding constant and

ΔH : change in enthalpy of binding

The heat corresponding to the i^{th} injection only, $\Delta Q(i)$, is equal to the difference between $Q(i)$ and $Q(i - 1)$ and is given by Eq. 1, which involves the necessary correction factor for the displaced volume (the injection volume dV_i):

$$\Delta Q(i) = Q(i) + \frac{dV_i}{V} \left[\frac{Q(i) + Q(i-1)}{2} \right] - Q(i - 1) \quad (2)$$

Where

$\Delta Q(i)$: heat corresponding to the i^{th} injection

$Q(i)$: total heat evolved (or absorbed) during the binding process at the end of the i^{th} injection

$Q(i - 1)$: total heat evolved (or absorbed) during the binding process at the end of the

$(i - 1)^{\text{th}}$ injection

V : volume of the cell and

dV_i : displaced injection volume

The ITC unit measures the $\Delta Q(i)$ value for every injection. These values are then fitted to Eqs. 1 and 2 by a nonlinear least squares method using the data analysis program Origin® [MicroCal™]. The fit process is iterative, involving an initial guess of n , K_a , and ΔH , which allows calculating of $\Delta Q(i)$ values as mentioned above for all injections and comparing them with the corresponding experimentally determined values. Based on this comparison, the initial guess of n , K_a , and ΔH is improved, and the process is repeated until no further significant improvement in the fit can be obtained, ensuring the most accurate results possible.

Characterization of O-acyl L-alaninols

The homologous series of OAAOHs synthesized in the present study were characterized by various spectroscopic techniques. FTIR spectra of all samples were recorded using solid samples on a Nicolet iS5 FTIR spectrometer from Thermo Fisher Scientific. ^1H - and ^{13}C -NMR spectra were recorded on a Ascend™ 500 MHz FT-NMR spectrometer from Bruker. High-resolution mass spectra were obtained using a Maxis ESI-QTOF mass spectrometer from Bruker. The FTIR, ^1H -NMR, ^{13}C -NMR and high-resolution mass spectra of OMAOH are given in Figs. S1-S4 and the corresponding spectra of other OAAOHs are given in Figs. S5-S28. The FTIR spectrum of OMAOH given in Figure S1, shows the absorption band of ester carbonyl group at 1736 cm^{-1} , C-H stretching bands at $\sim 2848\text{-}2953 \text{ cm}^{-1}$, and C-O stretching bands at $\sim 1151 \text{ cm}^{-1}$. Methylene scissoring and rocking bands are seen at $\sim 1460 \text{ cm}^{-1}$ and $\sim 719 \text{ cm}^{-1}$, respectively. The IR spectra of the other OAAOHs are shown in Figs. S5-S10 and the important resonances are listed in Table S1.

A representative ^1H -NMR spectrum of OMAOH in CDCl_3 is given in Figure S2. OMAOH shows the following resonances: $\sim 0.88 \delta$ (3H,t), myristoyl terminal methyl group; $\sim 1.25 \delta$ (nH,m), all myristoyl chain methylene groups except those at α - and β - positions with respect to the carbonyl; $\sim 1.62 \delta$ (2H,m) for β -methylene w.r.t. carbonyl; $\sim 2.46 \delta$ (2H,t), α -methylene w.r.t. carbonyl; $\sim 3.62 \delta$ (1H,m), methine hydrogen in the alaninol moiety; $\sim 1.45 \delta$ (3H,d), methyl group in the alaninol moiety; $\sim 4.27 \delta$ (2H,m), methylene group of the alaninol moiety; $\sim 8.55 \delta$ (3H,bs), ammonium group. The ^1H -NMR spectra of the other OAAOHs are given in Figs. S11-S16 and the corresponding spectral data are listed in Table S2. The resonances in their spectra are also broadly similar to those described above for OMAOH except for the number of protons in the polymethylene chain.

A representative ^{13}C -NMR spectrum of OMAOH is given in Figure S3, which shows the following resonances: 14.12 and 15.24 δ for the acyl chain terminal methyl and methyl group in the polar region; 22.68 δ for the methylene α to the terminal methyl group; 24.69 δ for the methylene β to the carbonyl; 31.92 δ for the methylene α to the carbonyl; 34.0 δ for the methylene group α to the carbonyl; multiple resonances between 29.17 and 29.66 δ for the remaining methylene groups in the acyl chain; 47.5 δ for the methine carbon in the polar region; 64.31 δ for the methylene group connected to the ester oxygen; 173.51 δ for the carbonyl carbon. The ^{13}C -NMR of the remaining OAAOHs are shown in Figs. S17-S22 and the spectral data are listed in Table S3. The resonances in their spectra are also broadly similar to those described above for OMAOH except for the number of C atoms in the polymethylene chain.

A high-resolution mass spectrum of OMAOH is presented in Figure S4. The intense peak at $m/z=286.2748$ matches well with the compound molecular ion $[\text{M}+\text{H}]^+$ (calculated mass = 286.2746). The additional peaks at $m/z=571.5338$ have been assigned as $[\text{2M}+\text{H}]^+$ (calculated mass = 571.5336). The HRMS obtained for the homologous series of OAAOHs

are listed in Table S4 and the observed m/z values were found to be in excellent agreement with the calculated masses in all cases.

Table S1. Assignment of resonances in the IR spectra of *O*-acyl-L-alaninols. Values given are in wavenumbers (cm^{-1}).

Acyl chain length	C=O stretch (ester)	C-H stretch	C-C-O stretch	C-H scissoring	C-H rocking
14	~1736	~2848-2953	~1151	~1460	~719
15	~1731	~2848-2952	~1148	~1471	~719
16	~1731	~2848-2958	~1149	~1470	~718
17	~1730	~2848-2954	~1149	~1471	~718
18	~1730	~2848-2957	~1149	~1471	~717
19	~1742	~2849-2954	~1149	~1469	~718
20	~1730	~2848-2952	~1148	~1471	~720

Table S2. ^1H -NMR spectral data of *O*-acyl-L-alaninols in CDCl_3 solvent. Chemical shift values are given in ppm (δ scale). Protons corresponding to the resonances are shown in red.

Acyl chain length	$\text{CH}_3\text{-}(\text{CH}_2)_n$	$(\text{CH}_2)_n\text{-CH}_2\text{-C=O}$	$\text{O-CH}_2\text{-CH(CH}_3\text{)-NH}_3^+$	$\text{O-CH}_2\text{-CH(CH}_3\text{)-NH}_3^+$	$\text{O-CH}_2\text{-CH(CH}_3\text{)-NH}_3^+$	$\text{O-CH}_2\text{-CH(CH}_3\text{)-NH}_3^+$		
14	0.88, t	1.25, m	1.62, m	2.46, t	4.27, m	3.62, m	1.45, d	8.55
15	0.90, t	1.27, m	1.64, m	2.47, t	4.27, m	3.64, m	1.47, d	8.61
16	0.90, t	1.27, m	1.64, m	2.47, t	4.28, m	3.64, m	1.47, d	8.60
17	0.88, t	1.25, m	1.62, m	2.45, t	4.27, m	3.63, m	1.46, d	8.56
18	0.90, t	1.27, m	1.64, m	2.48, t	4.27, m	3.64, m	1.46, d	8.63
19	0.77, t	1.15, m	1.52, m	2.30, t	4.10, m	3.46, m	1.27, d	8.17
20	0.84, t	1.21, m	1.59, m	2.37, t	4.20, m	3.53, m	1.34, d	8.27

Table S3. ^{13}C -NMR spectral data of *O*-acyl-L-alaninols in CDCl_3 (solvent). Chemical shift values are given in ppm (δ scale). Carbon atoms corresponding to the resonances are shown in red.

Acyl chain length	$\text{CH}_3\text{-}$ $\text{CH}_2\text{-}$ $\text{CH}_2\text{-}$ (CH_2) _n	$\text{CH}_3\text{-}$ $\text{CH}_2\text{-}$ $\text{CH}_2\text{-}$ (CH_2) _n	(CH_2) _n	$\text{CH}_2\text{-}$ $\text{CH}_2\text{-}$ C=O	$\text{CH}_2\text{-}$ $\text{CH}_2\text{-}$ C=O	$\text{CH}_2\text{-}$ $\text{CH}(\text{CH}_3)\text{-}$ NH_3^+	$\text{CH}_2\text{-}$ $\text{CH}(\text{CH}_3)\text{-}$ NH_3^+	$\text{CH}_2\text{-}$ $\text{CH}(\text{CH}_3)$ NH_3^+	O- C=O	
n										
14	14.10	22.68	31.92	29.17- 29.66	24.69	34.00	64.31	47.50	15.24	173.51
15	14.10	22.68	31.92	29.17- 29.70	24.69	34.01	64.31	47.50	15.24	173.53
16	14.12	22.70	31.94	29.18- 29.72	24.69	34.02	64.32	47.52	15.25	173.58
17	14.11	22.69	31.93	29.18- 29.71	24.69	34.02	64.32	47.50	15.25	173.57
18	14.12	22.66	31.96	29.14- 29.78	24.81	33.93	64.53	46.87	15.16	173.78
19	13.94	22.57	31.82	29.04- 29.59	24.59	33.72	64.41	46.65	14.96	173.67
20	13.92	22.56	31.81	29.03- 29.58	24.59	33.72	64.41	46.67	14.96	173.65

Table S4. ESI-MS data of *O*-acyl-L-alaninols. Data (m/z values) are given for the peaks corresponding to molecular ion ($[\text{M}+\text{H}]^+$).

Acyl chain length	Theoretical m/z values	Experimental m/z values	Assignment
14	286.2746	286.2756	$[\text{M}+\text{H}]^+$
15	300.2902	300.2908	$[\text{M}+\text{H}]^+$
16	314.3059	314.3051	$[\text{M}+\text{H}]^+$
17	328.3215	328.3224	$[\text{M}+\text{H}]^+$
18	342.3372	342.3372	$[\text{M}+\text{H}]^+$
19	356.3528	356.3558	$[\text{M}+\text{H}]^+$
20	370.3685	370.3676	$[\text{M}+\text{H}]^+$

Table S5. Average values of transition temperatures (T_t), transition enthalpies (ΔH_t) and transition entropies (ΔS_t) of OAAOHs in dry and hydrated states. Samples were hydrated in 150 mM NaCl. Values in parentheses correspond to standard deviations from three independent measurements.

Acyl		Dry OAAOHs			Hydrated OAAOHs		
chain	length	T_t (°C)	ΔH_t (kcal.mol ⁻¹)	ΔS_t (cal.mol ⁻¹ .K ⁻¹)	T_t (°C)	ΔH_t (kcal.mol ⁻¹)	ΔS_t (cal.mol ⁻¹ .K ⁻¹)
14	104.4 (0.1)	7.72 (0.42)	20.45 (1.11)	15.8 (0.2)	3.19 (0.27)	10.95 (0.78)	
15	106.2 (0.1)	8.65 (0.51)	22.81 (1.35)	28.2 (0.2)	3.55 (0.04)	11.85 (0.07)	
16	108.1 (0.0)	9.14 (0.47)	23.96 (1.22)	38.4 (0.5)	3.61 (0.26)	11.60 (0.85)	
17	109.4 (0.1)	10.75 (0.16)	28.10 (0.43)	46.4 (0.2)	4.13 (0.23)	12.47 (1.05)	
18	110.5 (0.2)	10.92 (0.34)	28.46 (0.88)	52.7 (0.6)	4.41 (0.30)	13.67 (1.01)	
19	112.8 (0.2)	12.27 (0.46)	31.79 (1.19)	59.3 (0.2)	4.84 (0.02)	14.53 (0.06)	
20	113.9 (0.2)	12.52 (0.54)	32.34 (1.39)	64.5 (0.1)	5.25 (0.29)	15.53 (0.85)	

Table S6. Fractional atomic coordinates ($\times 10^4$) and equivalent isotropic displacement parameters ($\text{\AA}^2 \times 10^3$) of OPAOH. U(eq) is defined as one third of the trace of the orthogonalized U_{ij} tensor. [$U(\text{eq}) = \frac{1}{3} \sum_i \sum_j U_{ij} a_i^* a_j^* a_i a_j \cos(a_i, a_j)$].

Atom	x	y	z	U(eq)
C11	-1920.2(11)	3953(2)	4540.1(3)	63.1(4)
O1	-545(5)	5185(7)	6552.1(18)	133(2)
O2	-692(4)	2572(5)	6268.7(9)	60.1(8)
N1	-1591(4)	2818(5)	5448.7(10)	53.6(9)
C1	51(5)	3826(9)	6482.1(14)	64.7(12)
C2	1664(5)	3317(7)	6586.6(14)	62.8(14)
C3	2339(5)	4394(7)	6934.2(14)	61.3(14)
C4	4012(5)	3972(9)	7016.3(13)	61.4(11)
C5	4724(6)	4982(8)	7366.9(14)	65.5(14)
C6	6387(5)	4489(7)	7453.5(15)	65.3(14)
C7	7125(6)	5452(8)	7805.6(15)	67.2(14)
C8	8788(6)	4982(8)	7885.9(16)	69.5(15)
C9	9520(6)	5916(9)	8239.5(15)	72.6(15)
C10	11182(6)	5452(9)	8319.2(15)	75.1(16)
C11	11915(6)	6397(9)	8674.3(16)	77.1(16)
C12	13567(6)	5911(9)	8758.6(17)	80.5(17)
C19	-4083(5)	4040(11)	5629.5(15)	74.4(14)
C18	-2408(4)	3877(8)	5757.2(12)	54.0(10)
C13	14278(6)	6858(9)	9118.8(17)	86.2(19)
C14	15938(7)	6370(10)	9212.3(19)	92(2)
C15	16651(7)	7331(13)	9560.7(19)	119(3)
C16	18281(8)	6856(16)	9660(2)	145(4)
C17	-2269(5)	2940(8)	6153.7(14)	62.9(13)

Table S7. Bond lengths and bond angles of OPAOH.

Bond lengths (\AA)		Bond angles (degrees)	
N(1)-C(18)	1.495(5)	N(1)-C(18)-C(19)	108.7(4)
O(2)- C(1)	1.345(7)	N(1)-C(18)-C(17)	108.5(4)
O(2)- C(17)	1.446(5)	O(2)-C(17)-C(18)	112.4(4)
O(1)- C(1)	1.181(7)	O(2)-C(1)-C(2)	112.3(5)
C(1)- C(2)	1.490(6)	O(1)-C(1)-C(2)	126.6(5)
C(2)- C(3)	1.523(6)	O(1)-C(1)-O(2)	120.9(4)
C(3)- C(4)	1.511(5)	C(1)-O(2)-C(17)	116.5(4)
C(4)- C(5)	1.516(6)	C(1)-C(2)-C(3)	112.6(4)
C(5)- C(6)	1.517(6)	C(2)-C(3)-C(4)	112.2(4)
C(6)- C(7)	1.511(6)	C(3)-C(4)-C(5)	114.1(4)
C(7)- C(8)	1.511(6)	C(4)-C(5)-C(6)	113.2(4)
C(8)- C(9)	1.503(7)	C(5)-C(6)-C(7)	114.6(4)
C(9)- C(10)	1.507(7)	C(6)-C(7)-C(8)	114.4(5)
C(10)- C(11)	1.511(7)	C(7)-C(8)-C(9)	114.6(5)
C(11)- C(12)	1.506(7)	C(8)-C(9)-C(10)	114.6(5)
C(12)- C(13)	1.517(7)	C(9)-C(10)-C(11)	114.5(5)
C(13)- C(14)	1.519(7)	C(10)-C(11)-C(12)	114.5(5)
C(14)- C(15)	1.493(8)	C(11)-C(12)-C(13)	113.7(5)
C(15)- C(16)	1.494(9)	C(12)-C(13)-C(14)	114.6(5)
C(17)- C(18)	1.500(7)	C(13)-C(14)-C(15)	114.7(6)
C(18)- C(19)	1.516(5)	C(14)-C(15)-C(16)	115.5(7)
		C(17)-C(18)-C(19)	110.1(4)

Table S8. Torsion angles (degrees) for OPAOH.

N1	C18	C17	O2	54.6(5)
C19	C18	C17	O2	173.5(4)
C18	C17	O2	C1	89.0(5)
C17	O2	C1	O1	-3.6(7)
C17	O2	C1	C2	179.8(4)
O2	C1	C2	C3	-161.0(4)
O1	C1	C2	C3	22.6(8)
C1	C2	C3	C4	-175.4(4)
C2	C3	C4	C5	-178.6(4)
C3	C4	C5	C6	177.9(4)
C4	C5	C6	C7	-179.1(4)
C5	C6	C7	C8	-178.9(4)
C6	C7	C8	C9	-179.1(4)
C7	C8	C9	C10	-179.8(5)
C8	C9	C10	C11	179.8(5)
C9	C10	C11	C12	178.9(5)
C10	C11	C12	C13	-179.4(5)
C11	C12	C13	C14	179.3(5)
C12	C13	C14	C15	178.6(5)
C13	C14	C15	C16	179.4(6)

Table S9. Fractional atomic coordinates ($\times 10^4$) and equivalent isotropic displacement parameters ($\text{\AA}^2 \times 10^3$) of OHDAOH. U(eq) is defined as one third of the trace of the orthogonalized U_{ij} tensor. [$U(\text{eq}) = \frac{1}{3} \sum_i \sum_j U_{ij} a_i^* a_j^* a_i a_j \cos(a_i, a_j)$].

Atom	x	y	z	U(eq)
Cl1	1662.5(8)	-7508.1(14)	4527.5(3)	57.4(3)
O1	867(3)	-5147(4)	6318.3(11)	90.8(11)
O2	3091(3)	-6278(4)	6259.1(9)	69.4(9)
N1	1727(3)	-6395(4)	5420.1(9)	52.2(8)
C1	2172(4)	-5019(5)	6377.9(12)	54.4(10)
C2	3004(4)	-3524(5)	6585.6(13)	60.6(11)
C3	2059(4)	-2098(5)	6755.5(12)	59.6(12)
C4	2967(4)	-704(5)	6992.2(12)	58.3(10)
C5	2097(4)	798(5)	7157.5(13)	62.8(11)
C6	3019(4)	2180(5)	7393.1(13)	62.1(11)
C7	2154(4)	3685(5)	7568.0(14)	65.3(11)
C8	3101(4)	5055(6)	7804.5(14)	67.3(12)
C9	2236(4)	6548(6)	7980.0(14)	68.5(12)
C10	3184(4)	7914(5)	8216.1(14)	69.7(13)
C11	2343(4)	9387(6)	8399.7(14)	72.5(13)
C12	3283(5)	10751(6)	8635.6(14)	76.2(13)
C13	2439(5)	12249(7)	8818.3(14)	78.6(13)
C14	3383(6)	13565(6)	9061.2(15)	86.9(15)
C15	2563(6)	15083(7)	9243.1(16)	89.0(15)
C16	3512(6)	16367(8)	9488.9(19)	117(2)
C17	2710(7)	17831(8)	9681(2)	144(3)
C18	2469(5)	-7835(5)	6059.3(13)	64.7(12)
C19	2680(3)	-7788(5)	5630.7(11)	49.9(9)
C20	4274(3)	-7487(7)	5544.6(12)	67.6(10)

Table S10. Bond lengths and bond angles of OHDAOH.

Bond lengths (Å)		Bong angles (Degrees)	
N(1)-C(19)	1.487(4)	N(1)-C(19)-C(20)	109.0(3)
O(2)-C(1)	1.338(4)	N(1)-C(19)-C(18)	111.6(3)
O(2)-C(18)	1.427(5)	O(2)-C(18)-C(19)	111.6(3)
O(1)-C(1)	1.185(4)	O(2)-C(1)-C(2)	111.2(3)
C(1)- C(2)	1.482(5)	O(1)-C(1)-O(2)	122.1(4)
C(2)- C(3)	1.510(5)	O(1)-C(1)-C(2)	126.7(4)
C(3)- C(4)	1.507(5)	C(1)-O(2)-C(18)	118.5(3)
C(4)- C(5)	1.504(5)	C(1)-C(2)-C(3)	115.1(3)
C(5)- C(6)	1.505(5)	C(2)-C(3)-C(4)	112.5(3)
C(6)- C(7)	1.517(5)	C(3)-C(4)-C(5)	115.3(3)
C(7)- C(8)	1.512(5)	C(4)-C(5)-C(6)	114.7(3)
C(8)- C(9)	1.511(5)	C(5)-C(6)-C(7)	115.3(3)
C(9)- C(10)	1.510(5)	C(6)-C(7)-C(8)	114.4(3)
C(10)- C(11)	1.501(5)	C(7)-C(8)-C(9)	114.3(3)
C(11)- C(12)	1.505(5)	C(8)-C(9)-C(10)	114.2(3)
C(12)- C(13)	1.514(6)	C(9)-C(10)-C(11)	115.0(3)
C(13)- C(14)	1.495(6)	C(10)-C(11)-C(12)	115.2(3)
C(14)- C(15)	1.512(6)	C(11)-C(12)-C(13)	115.4(3)
C(15)- C(16)	1.487(6)	C(12)-C(13)-C(14)	114.9(3)
C(16)- C(17)	1.492(7)	C(13)-C(14)-C(15)	115.7(4)
C(18)- C(19)	1.493(5)	C(14)-C(15)-C(16)	115.2(4)
C(19)- C(20)	1.518(4)	C(15)-C(16)-C(17)	115.6(5)
		C(18)-C(19)-C(20)	113.8(3)

Table S11. Torsion angles (degrees) for OHDAOH.

N1	C19	C18	O2	-71.2(4)
C20	C19	C18	O2	52.7(4)
C19	C18	O2	C1	107.5(4)
C18	O2	C1	O1	-0.9(6)
C18	O2	C1	C2	178.9(3)
O2	C1	C2	C3	-175.9(3)
O1	C1	C2	C3	3.8(6)
C1	C2	C3	C4	175.1(3)
C2	C3	C4	C5	177.8(3)
C3	C4	C5	C6	177.8(3)
C4	C5	C6	C7	-178.9(3)
C5	C6	C7	C8	179.8(3)
C6	C7	C8	C9	-179.7(3)
C7	C8	C9	C10	179.9(3)
C8	C9	C10	C11	-178.8(3)
C9	C10	C11	C12	179.9(3)
C10	C11	C12	C13	179.4(4)
C11	C12	C13	C14	178.3(4)
C12	C13	C14	C15	179.4(4)
C13	C14	C15	C16	179.1(4)
C14	C15	C16	C17	-177.9(5)

Table S12. Subcell dimensions of OPAOH and OHDAOH.

Cell parameter	OPAOH	OHDAOH
a (Å)	8.71	7.40
b (Å)	5.78	5.85
c (Å)	2.53	2.53

Table S13. Lamellar *d*-spacings of OAAOHs with different acyl chain lengths (number of C-atoms in the acyl chain, *n* = 14–20), derived from the powder X-ray diffraction measurements.

Chain length (<i>n</i>)	<i>d</i> -spacing
14	30.5 (0.1)
15	31.6 (0.2)
16	33.3 (0.4)
17	34.3 (0.3)
18	36.4 (0.4)
19	36.9 (0.3)
20	38.4 (0.2)

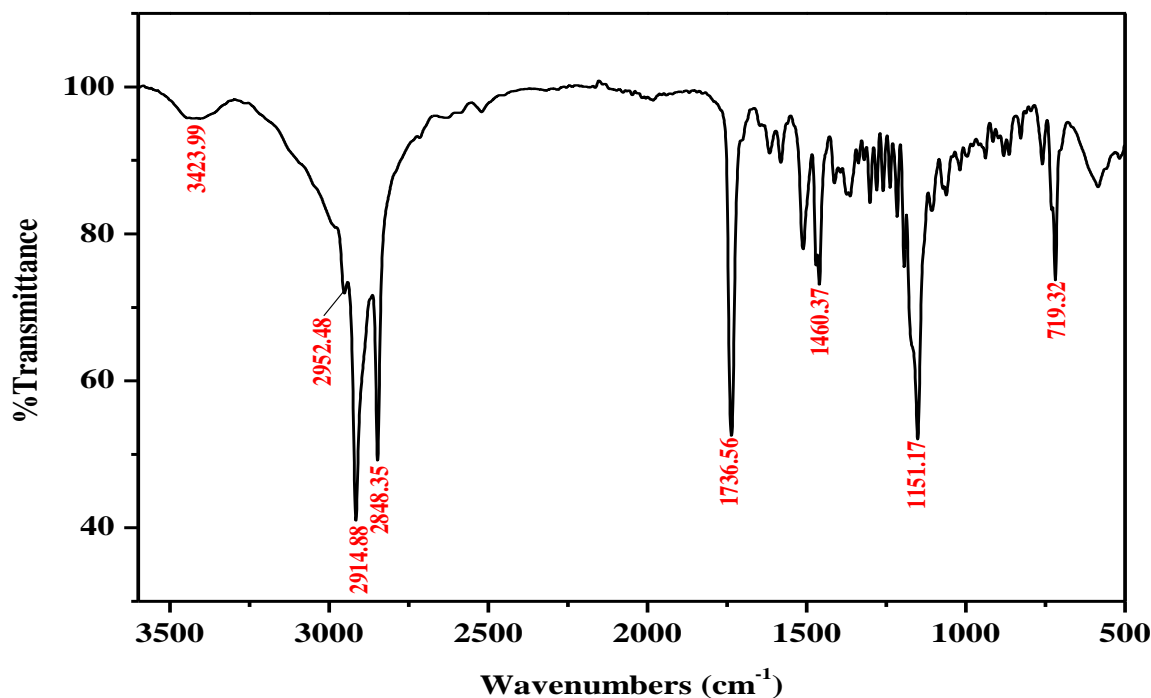


Figure S1. FTIR spectrum of *O*-myristoyl-L-alaninol recorded at room temperature.

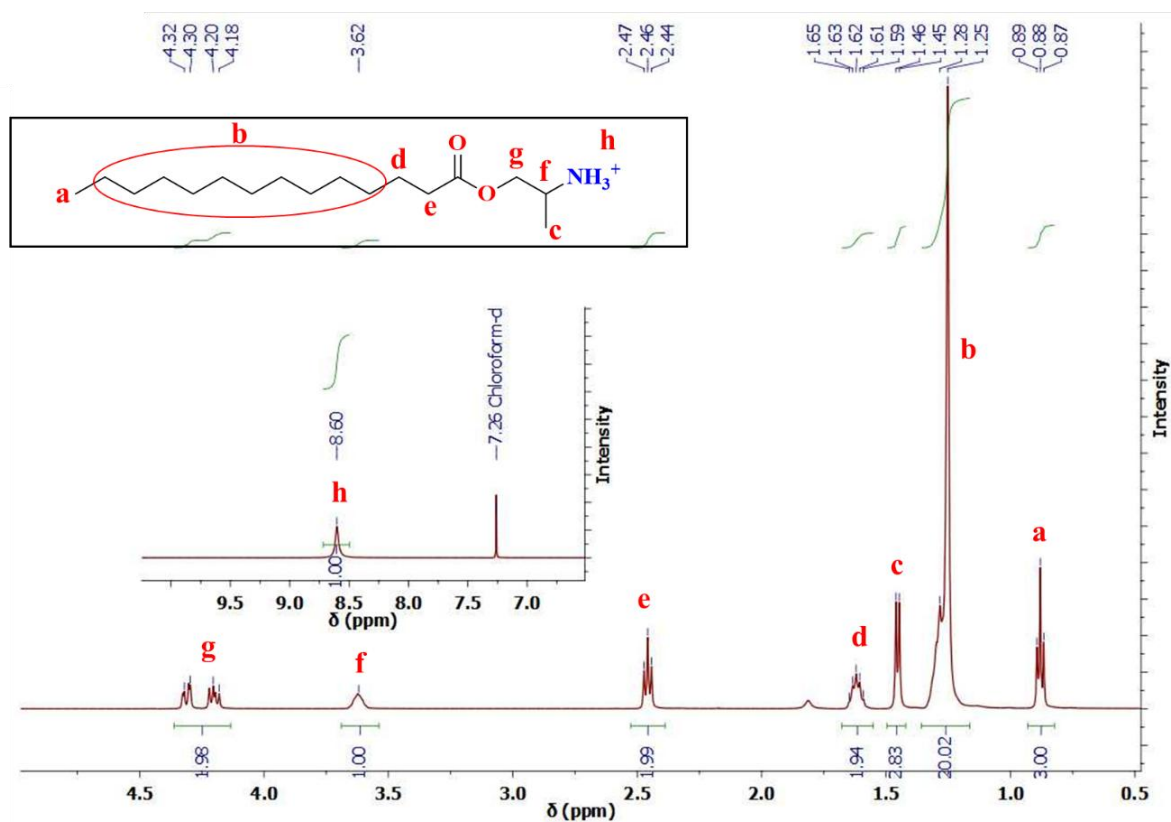


Figure S2. ¹H-NMR spectrum of *O*-myristoyl-L-alaninol recorded at room temperature (solvent CDCl_3).

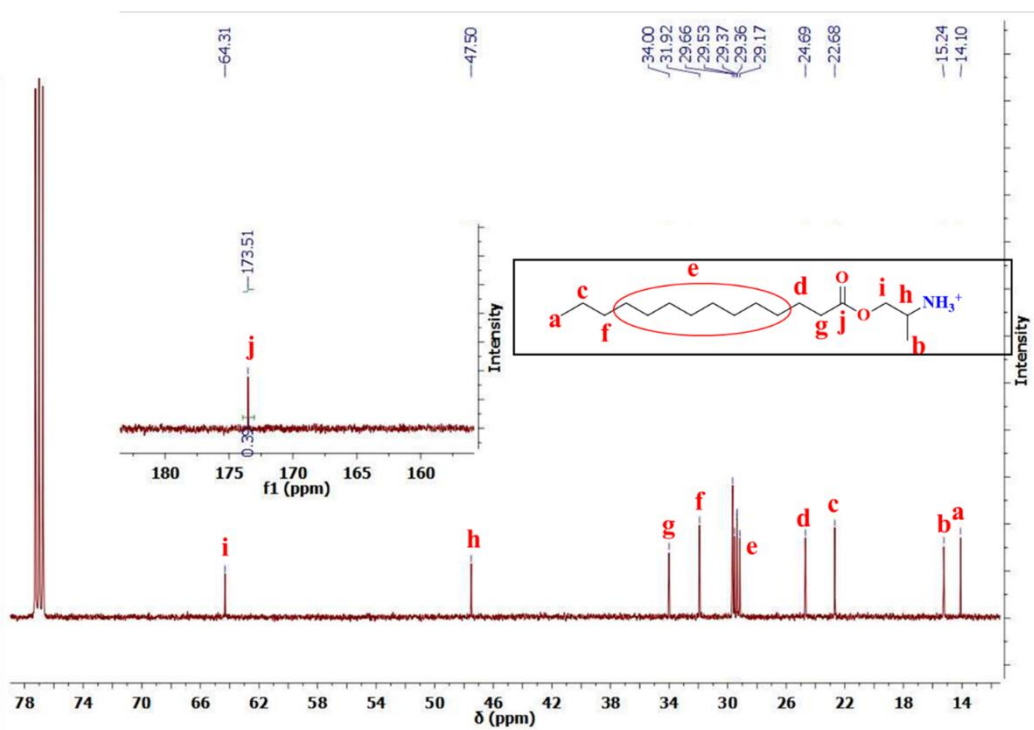


Figure S3. ^{13}C -NMR spectrum of *O*-myristoyl-L-alaninol recorded at room temperature (solvent CDCl_3).

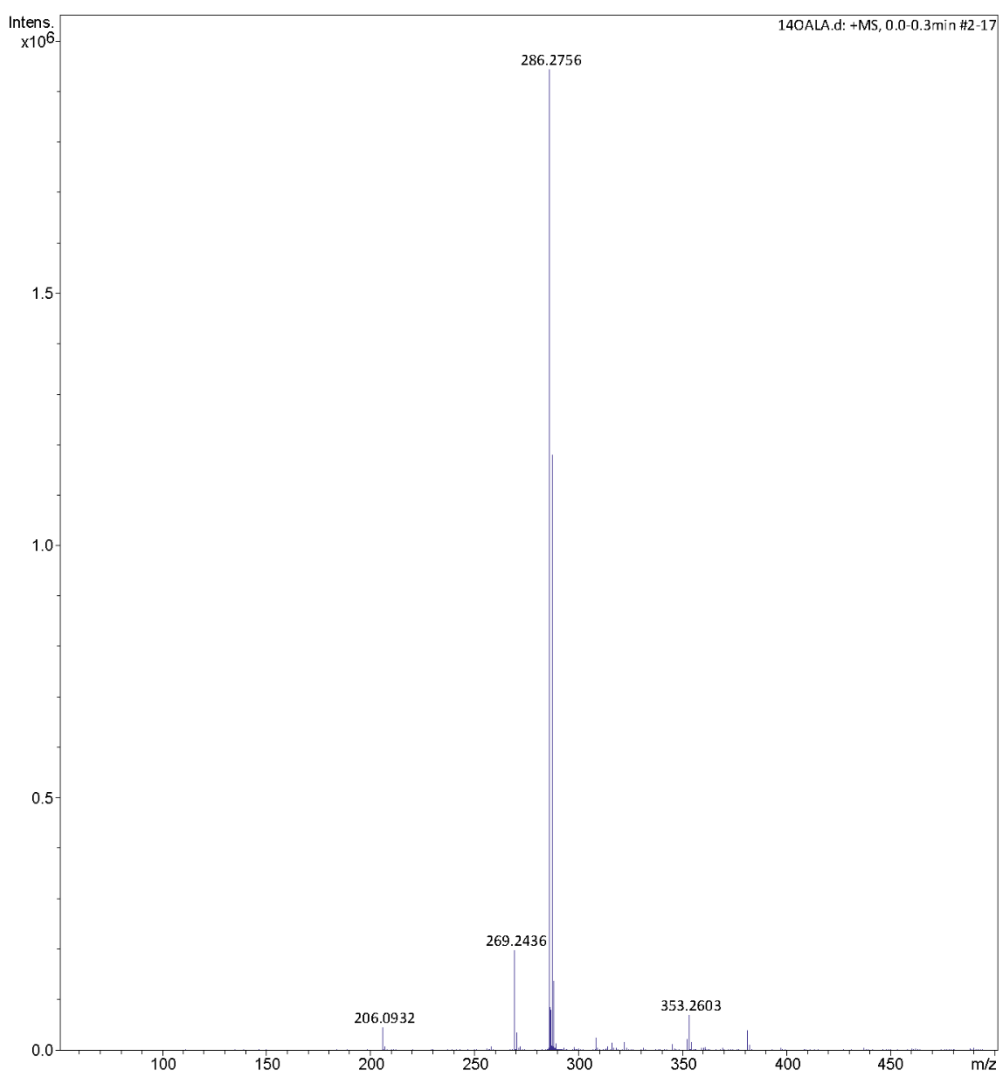


Figure S4. Electrospray ionisation (ESI) mass spectrum of *O*-myristoyl-L-alaninol.

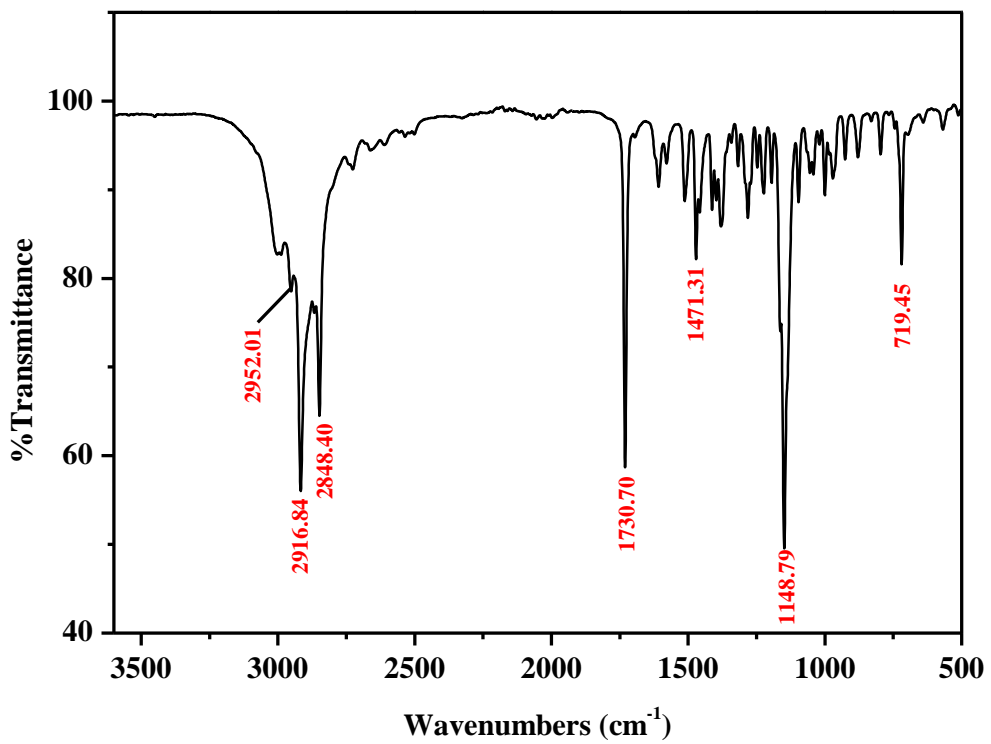


Figure S5. FTIR spectrum of *O*-pentadecanoyl-L-alaninol recorded at room temperature.

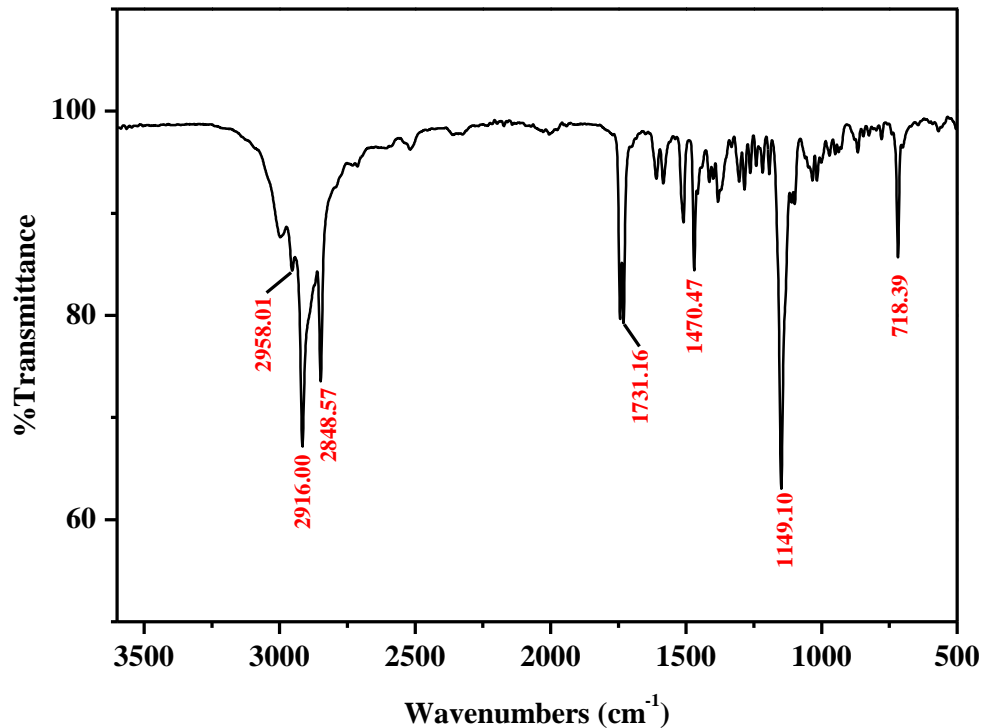


Figure S6. FTIR spectrum of *O*-palmitoyl-L-alaninol recorded at room temperature.

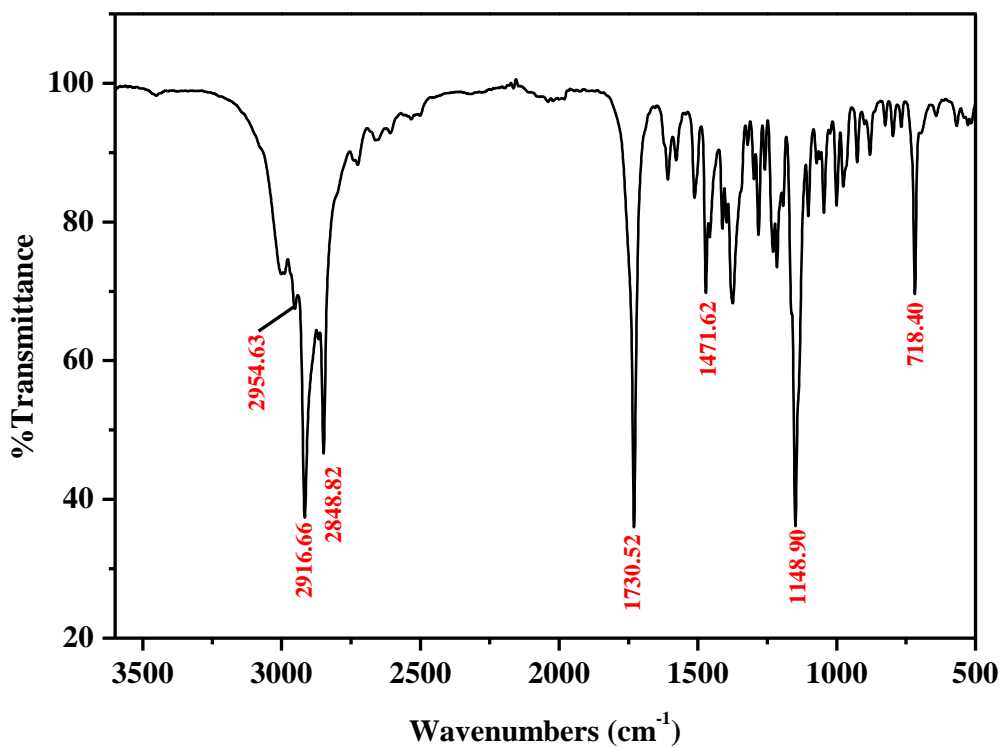


Figure S7. FTIR spectrum of *O*-heptadecanoyl-L-alaninol recorded at room temperature.

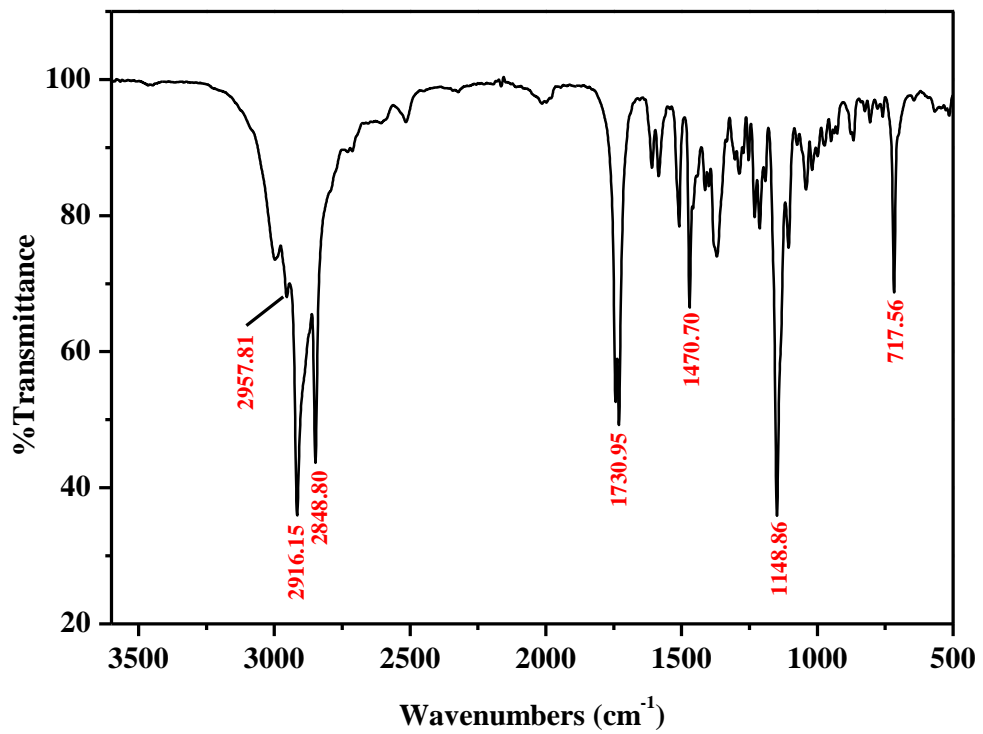


Figure S8. FTIR spectrum of *O*-stearoyl-L-alaninol recorded at room temperature.

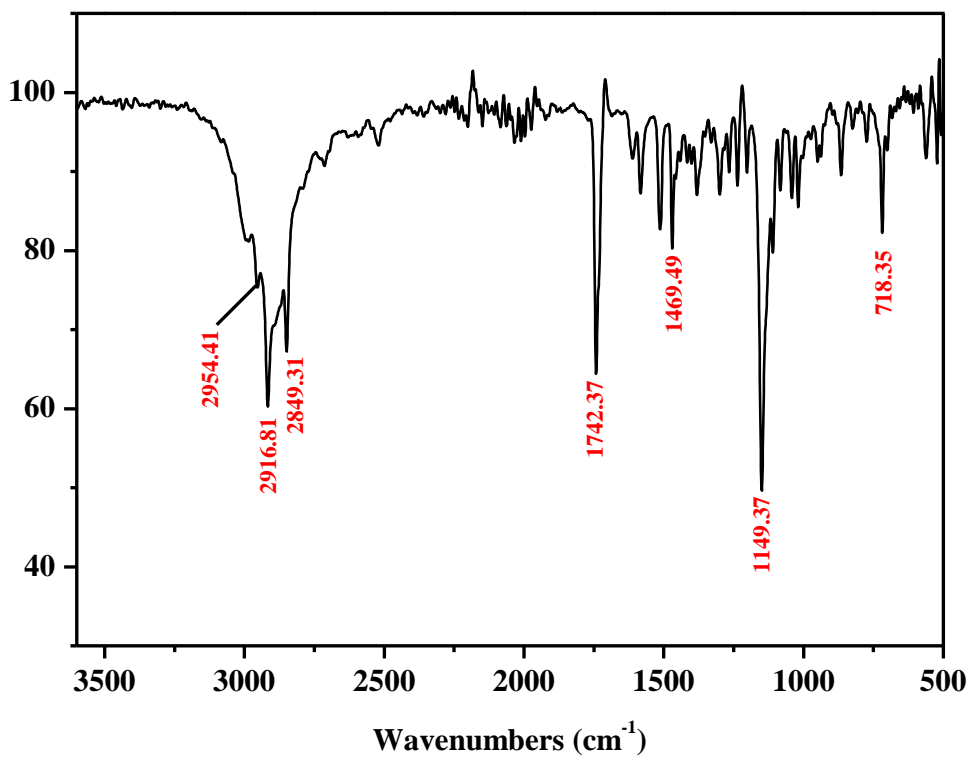


Figure S9. FTIR spectrum of *O*-nonadecanoyl-L-alaninol recorded at room temperature.

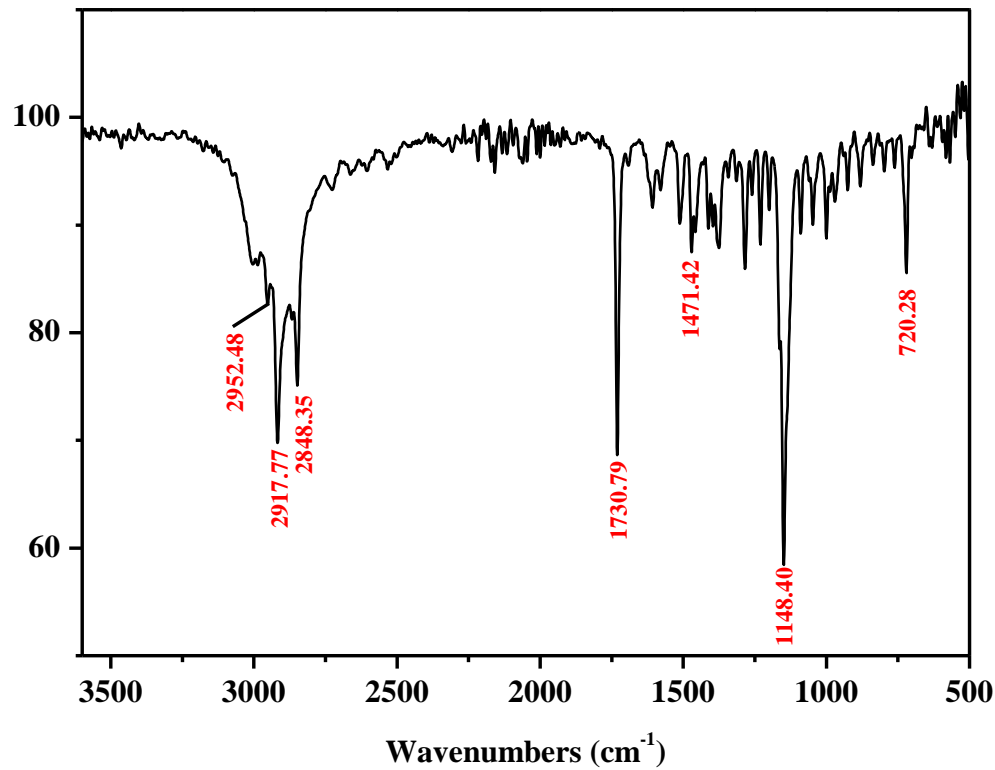


Figure S10. FTIR spectrum of *O*-eicosanoyl-L-alaninol recorded at room temperature.

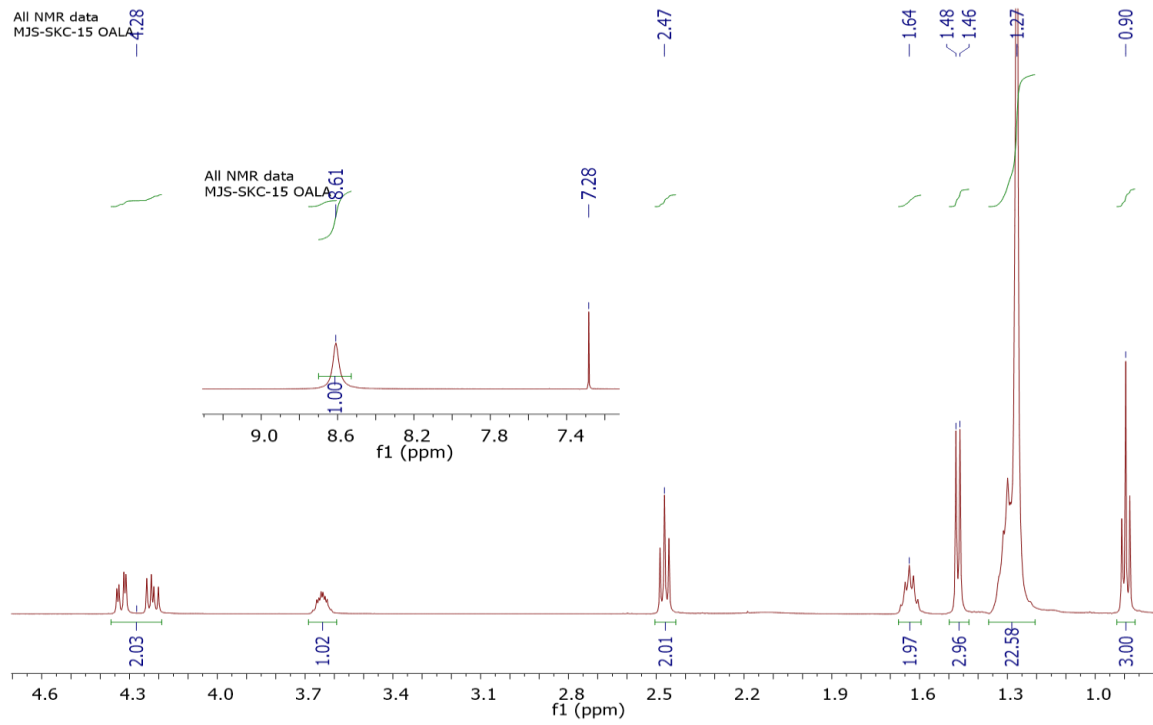


Figure S11. ¹H-NMR spectrum of *O*-pentadecanoyl-L-alaninol recorded at room temperature (solvent CDCl₃).

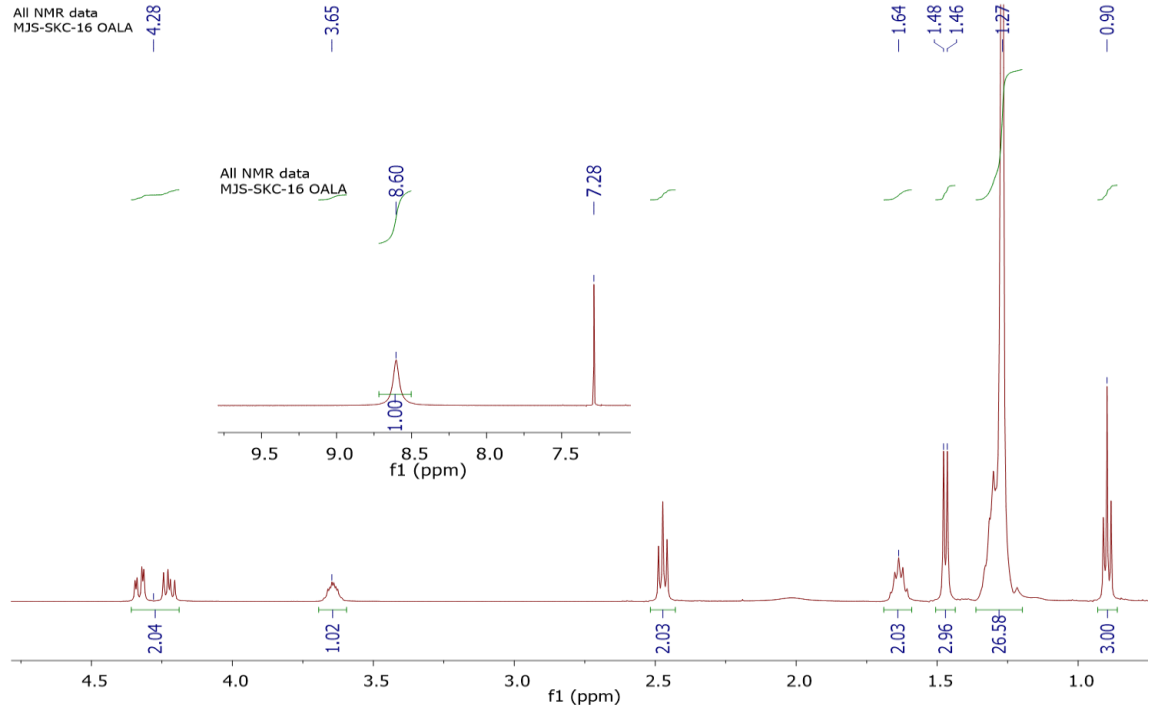


Figure S12. ¹H-NMR spectrum of *O*-palmitoyl-L-alaninol recorded at room temperature (solvent CDCl₃).

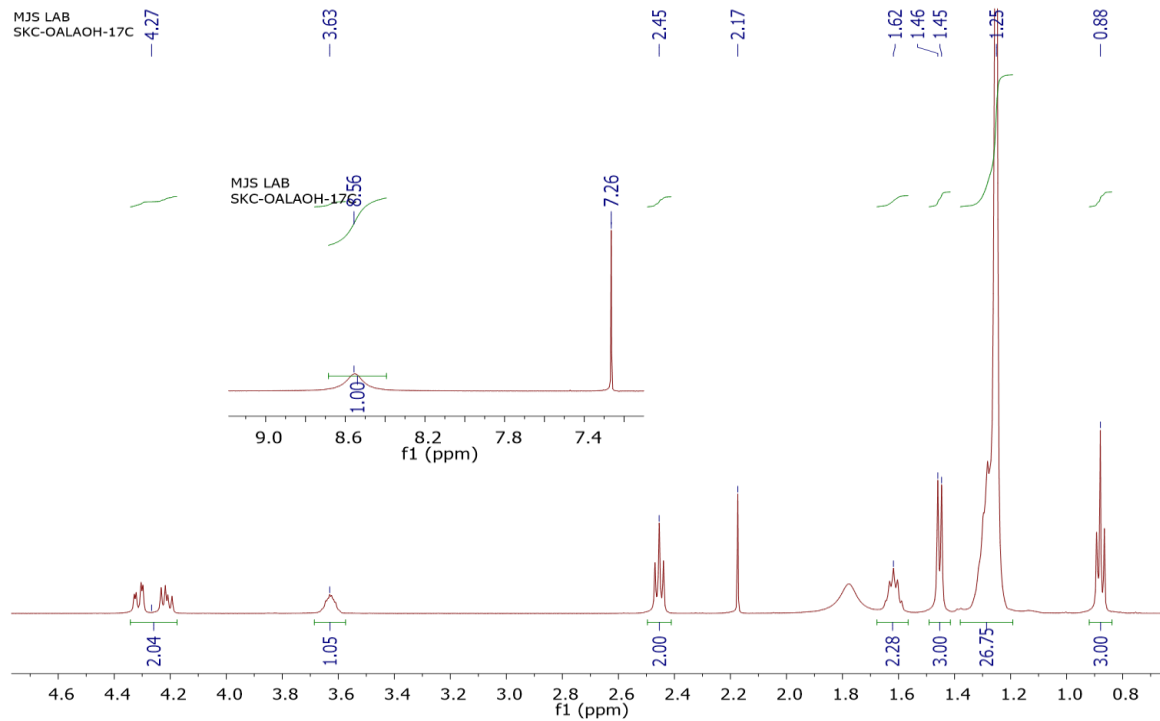


Figure S13. ¹H-NMR spectrum of *O*-heptadecanoyl-L-alaninol recorded at room temperature (solvent CDCl₃).

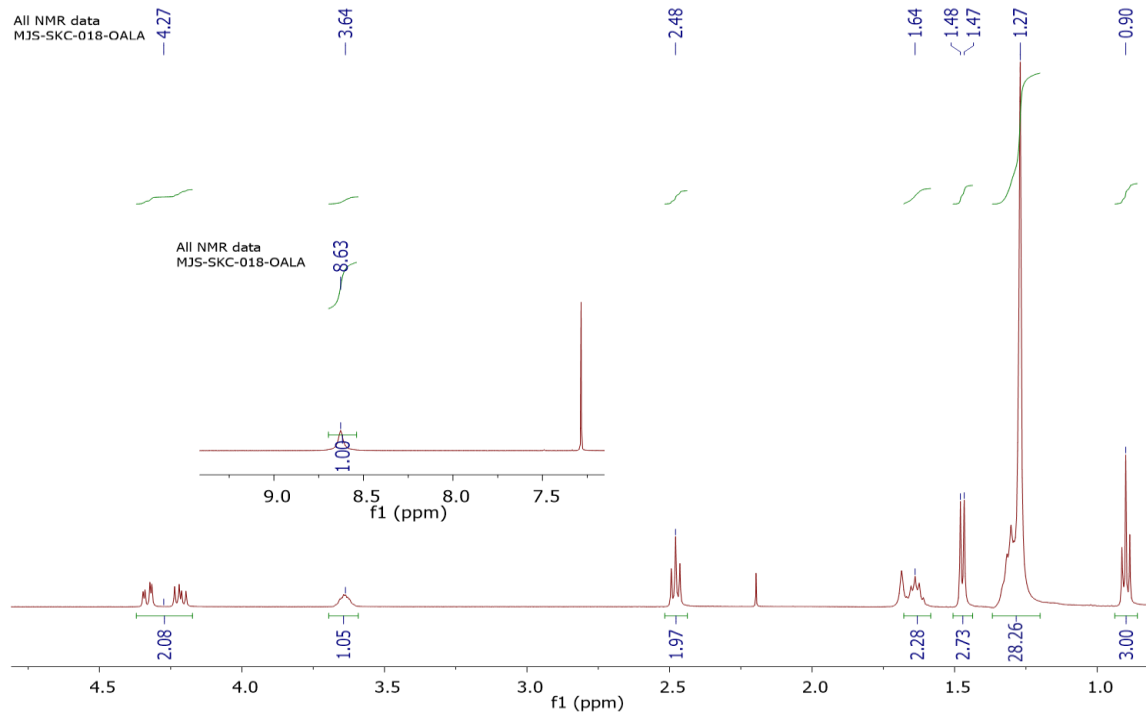


Figure S14. ¹H-NMR spectrum of *O*-stearoyl-L-alaninol recorded at room temperature (solvent CDCl₃).

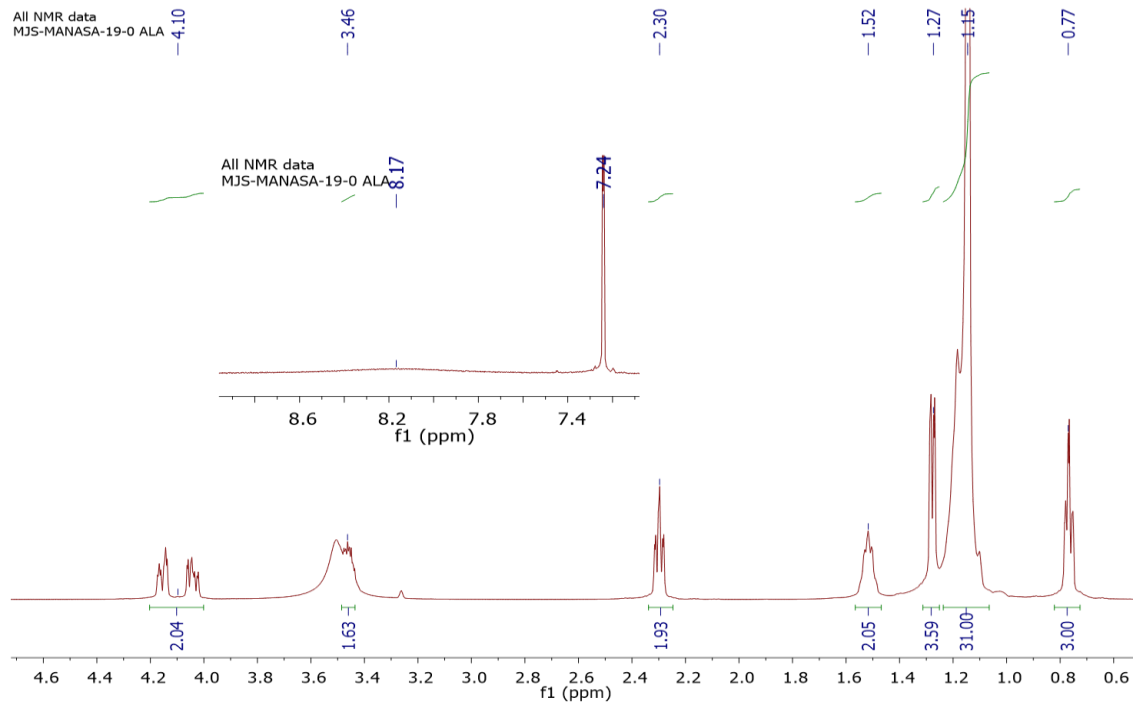


Figure S15. ^1H -NMR spectrum of *O*-nonadecanoyl-L-alaninol recorded at room temperature (solvent CDCl_3 +methanol- d_4).

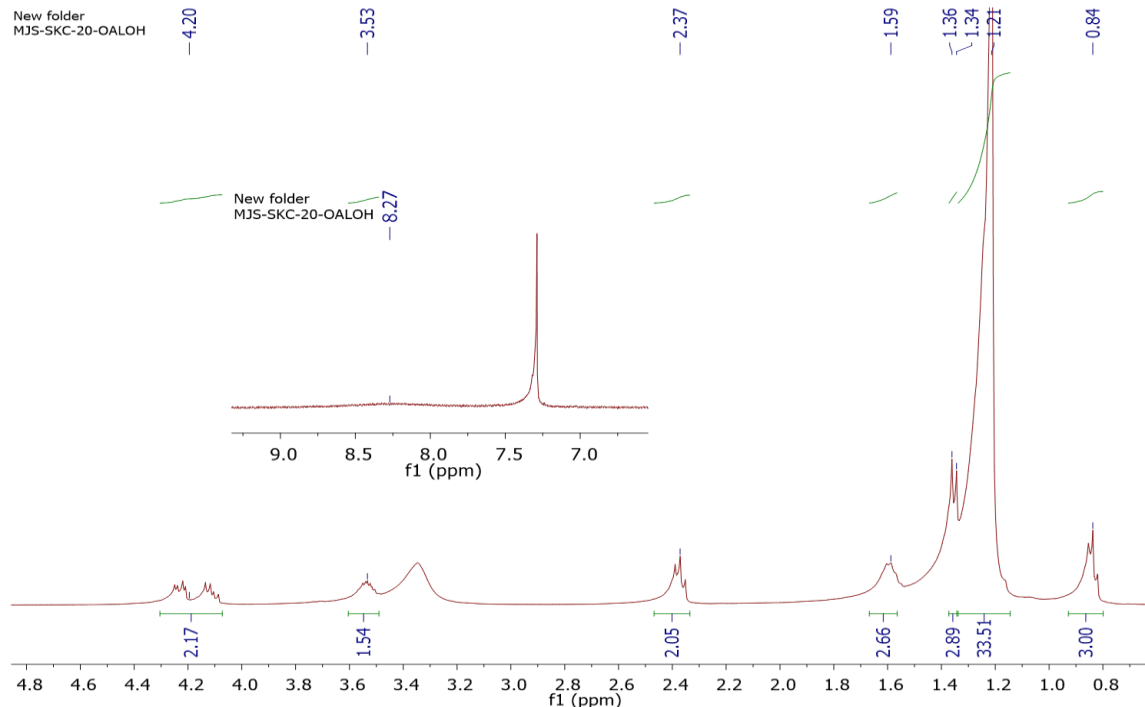


Figure S16. ^1H -NMR spectrum of *O*-eicosanoyl-L-alaninol recorded at room temperature (solvent CDCl_3 +methanol- d_4).

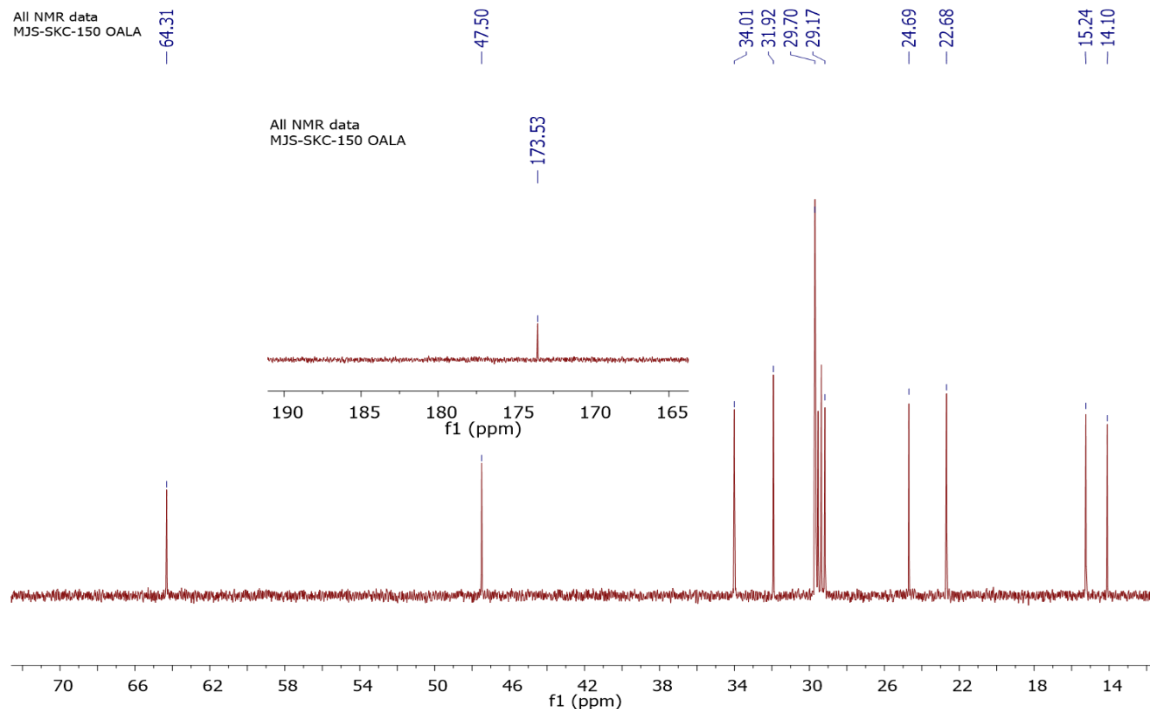


Figure S17. ^{13}C -NMR spectrum of *O*-pentadecanoyl-L-alaninol recorded at room temperature (solvent CDCl_3).

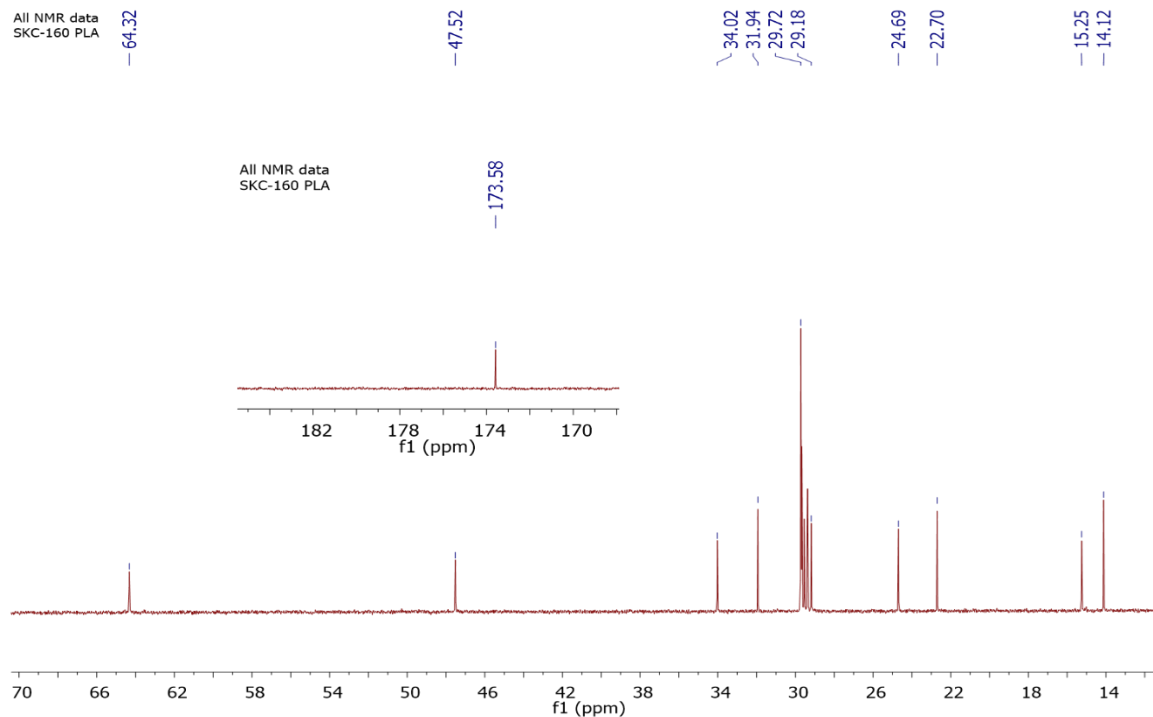


Figure S18. ^{13}C -NMR spectrum of *O*-palmitoyl-L-alaninol recorded at room temperature (solvent CDCl_3).

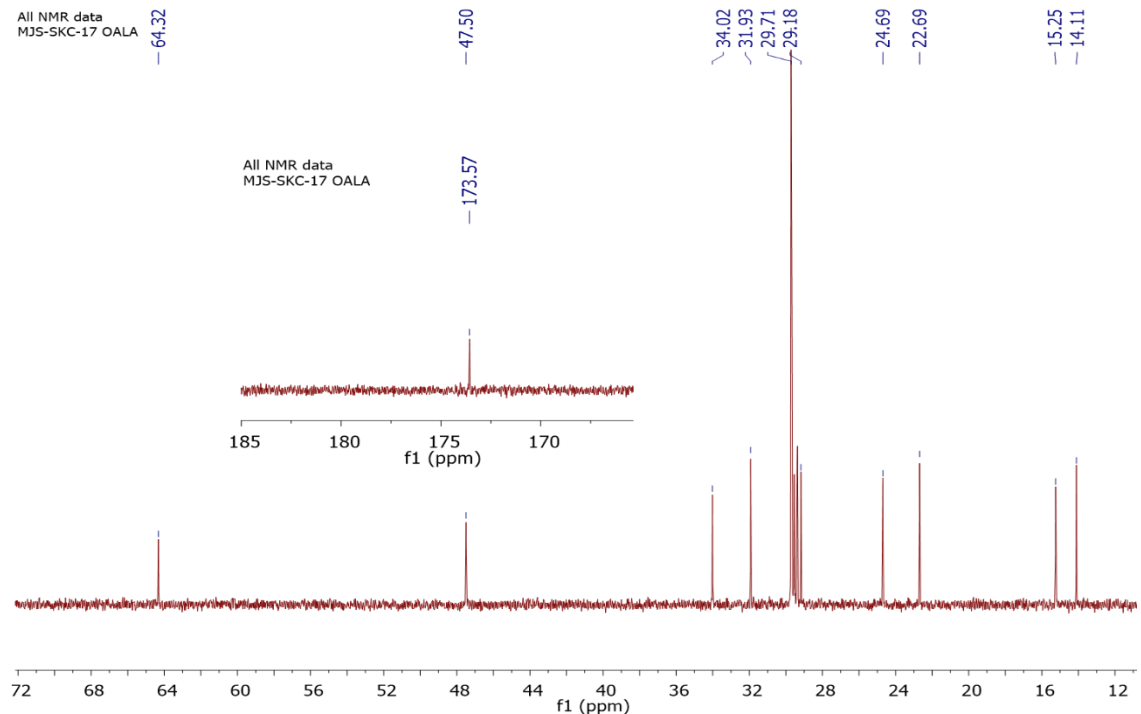


Figure S19. ^{13}C -NMR spectrum of *O*-heptadecanoyl-L-alaninol recorded at room temperature (solvent CDCl_3).

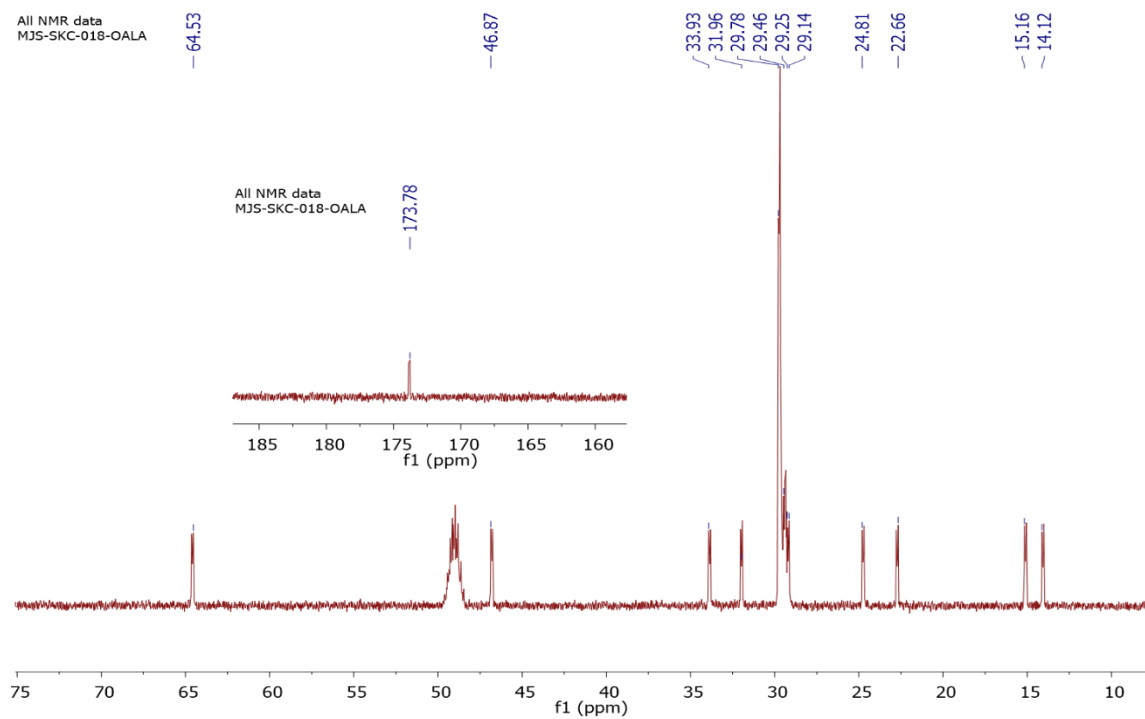


Figure S20. ^{13}C -NMR spectrum of *O*-stearoyl-L-alaninol recorded at room temperature (solvent $\text{CDCl}_3 + \text{methanol-d}_4$).

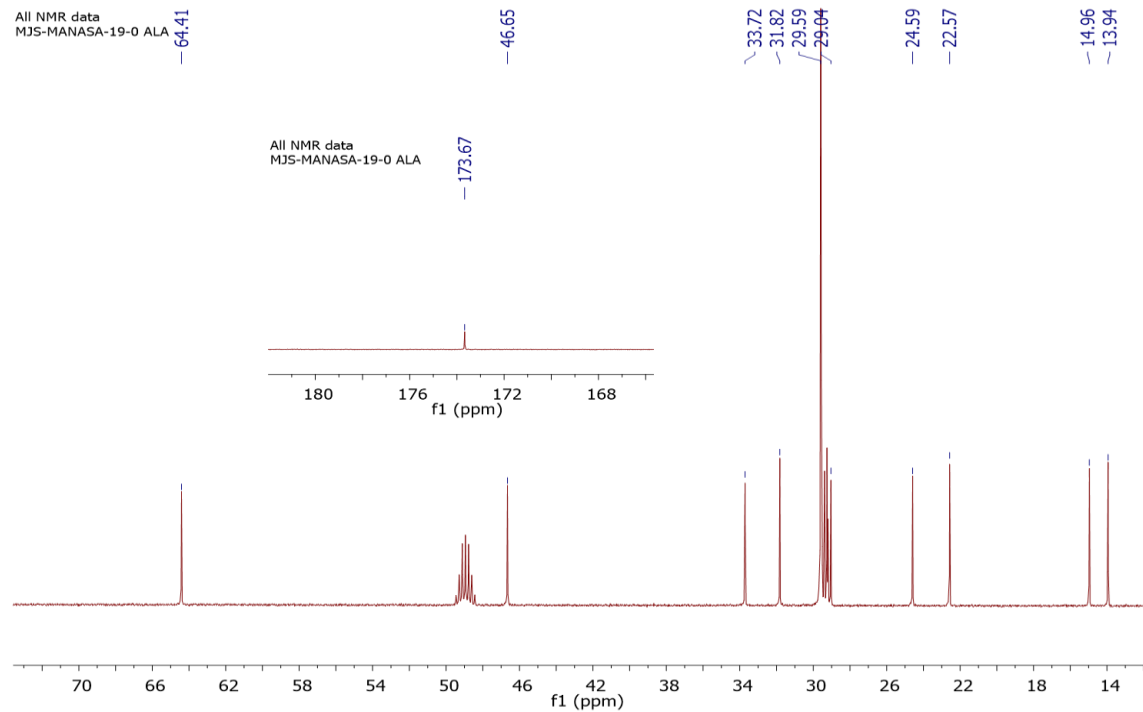


Figure S21. ^{13}C -NMR spectrum of *O*-nonadecanoyl-L-alaninol recorded at room temperature (solvent $\text{CDCl}_3 + \text{methanol-d}_4$).

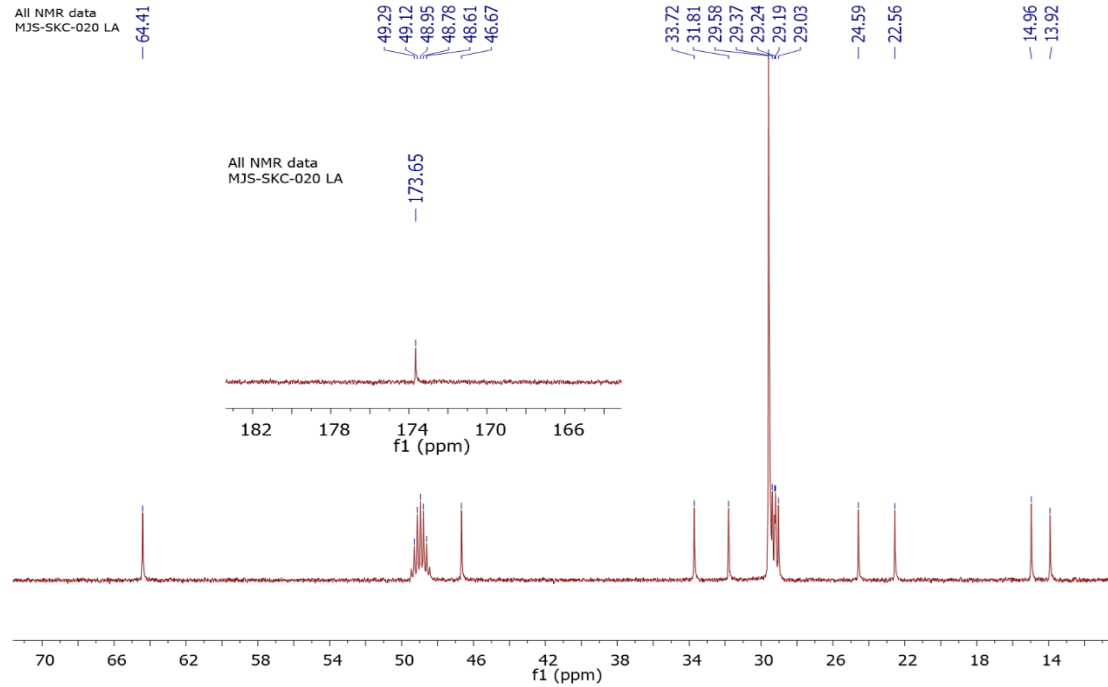


Figure S22. ^{13}C -NMR spectrum of *O*-eicosanoyl-L-alaninol recorded at room temperature (solvent $\text{CDCl}_3 + \text{methanol-d}_4$).

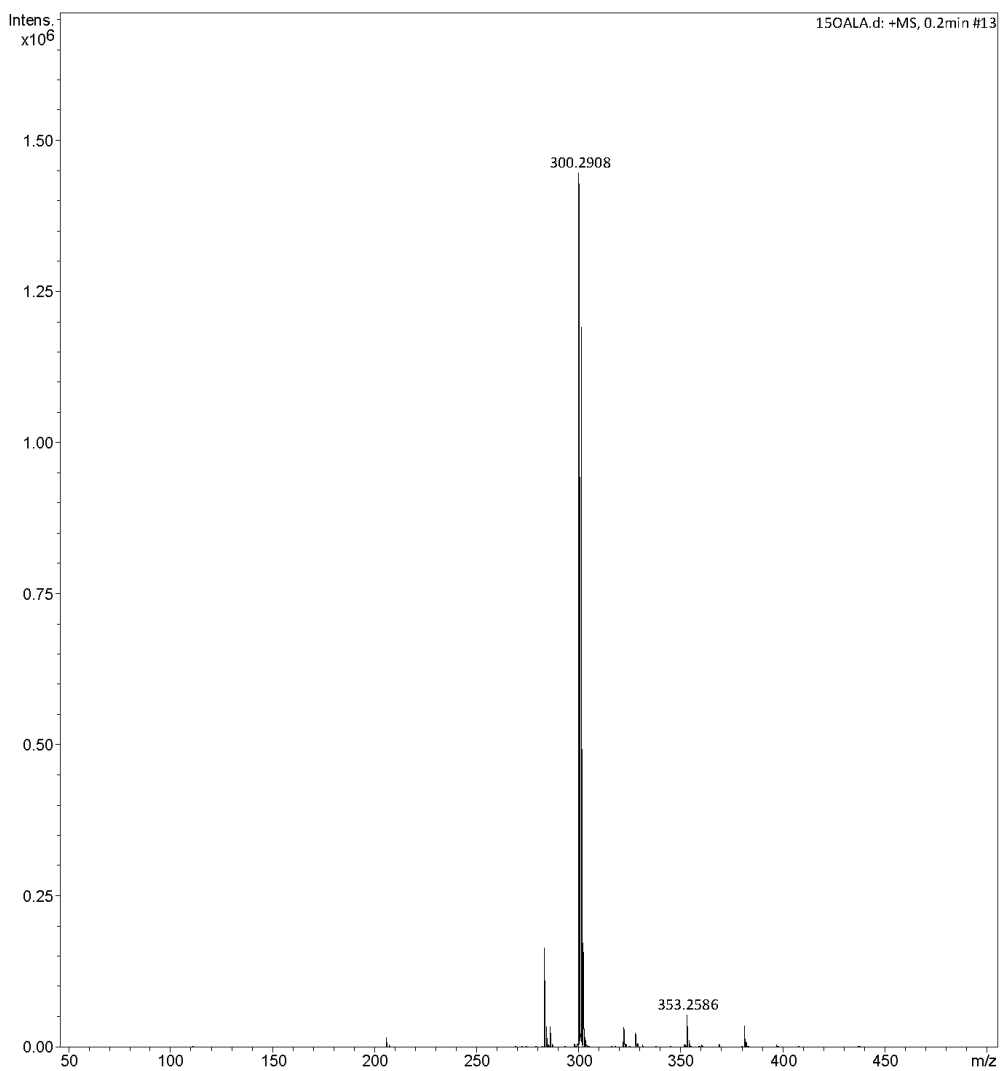


Figure S23. ESI mass spectrum of *O*-pentadecanoyl-L-alaninol.

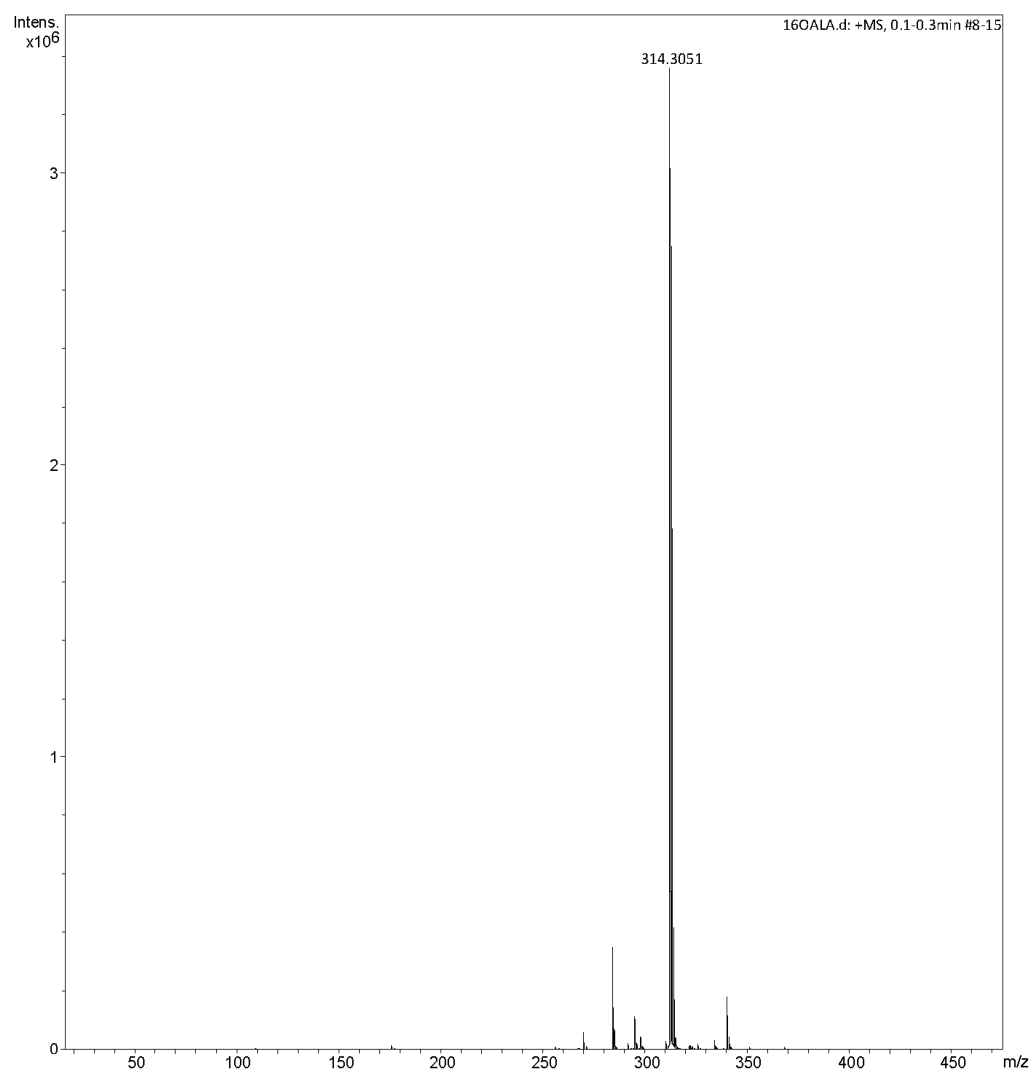


Figure S24. ESI mass spectrum of *O*-palmitoyl-L-alaninol.

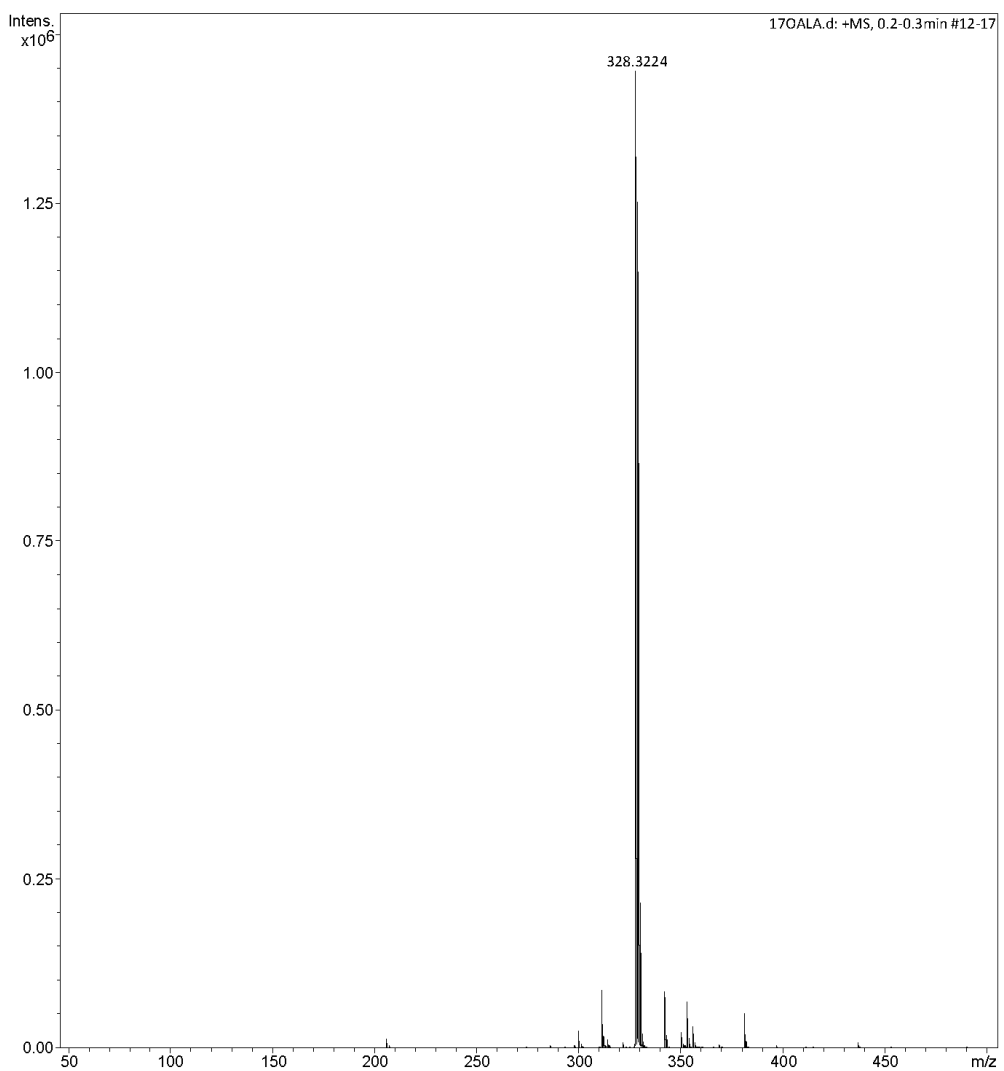


Figure S25. ESI mass spectrum of *O*-heptadecanoyl-L-alaninol.

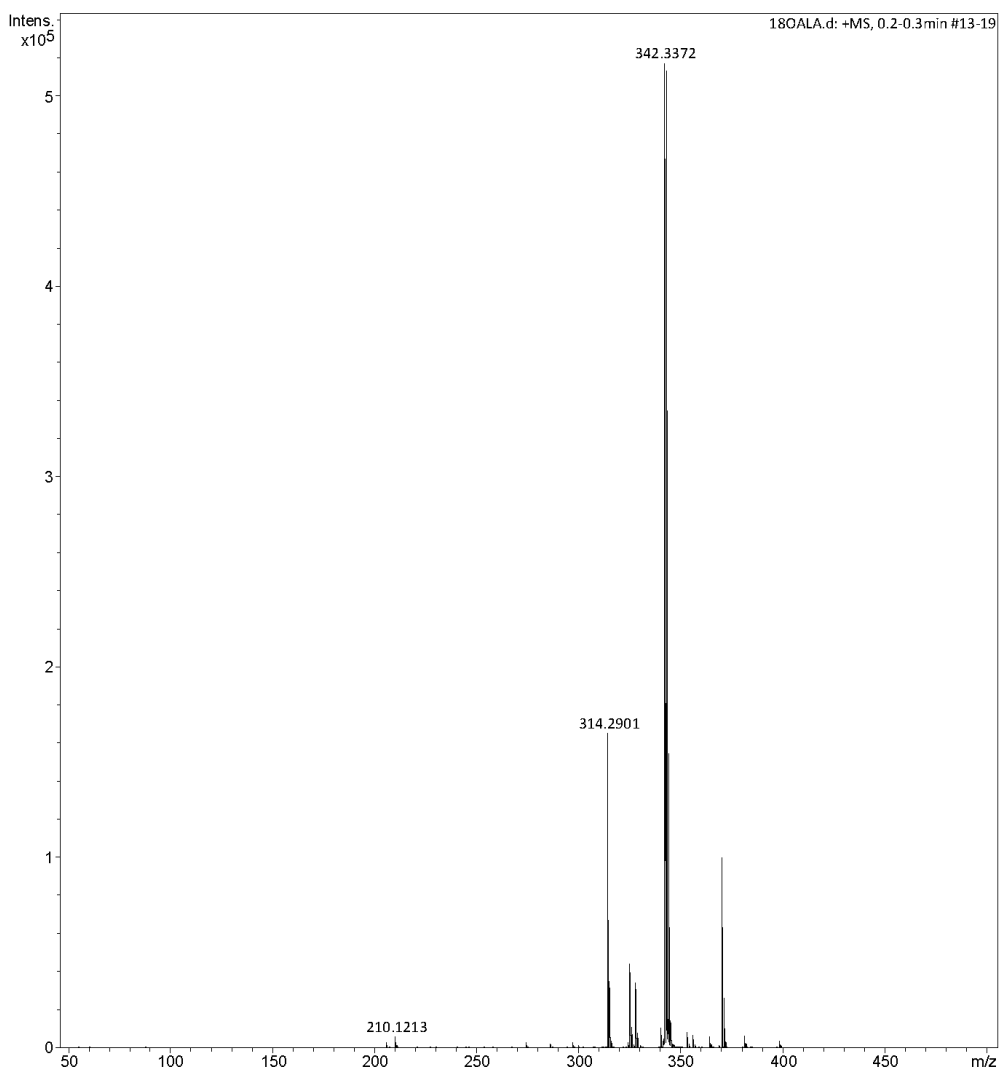


Figure S26. ESI mass spectrum of *O*-stearoyl-L-alaninol.

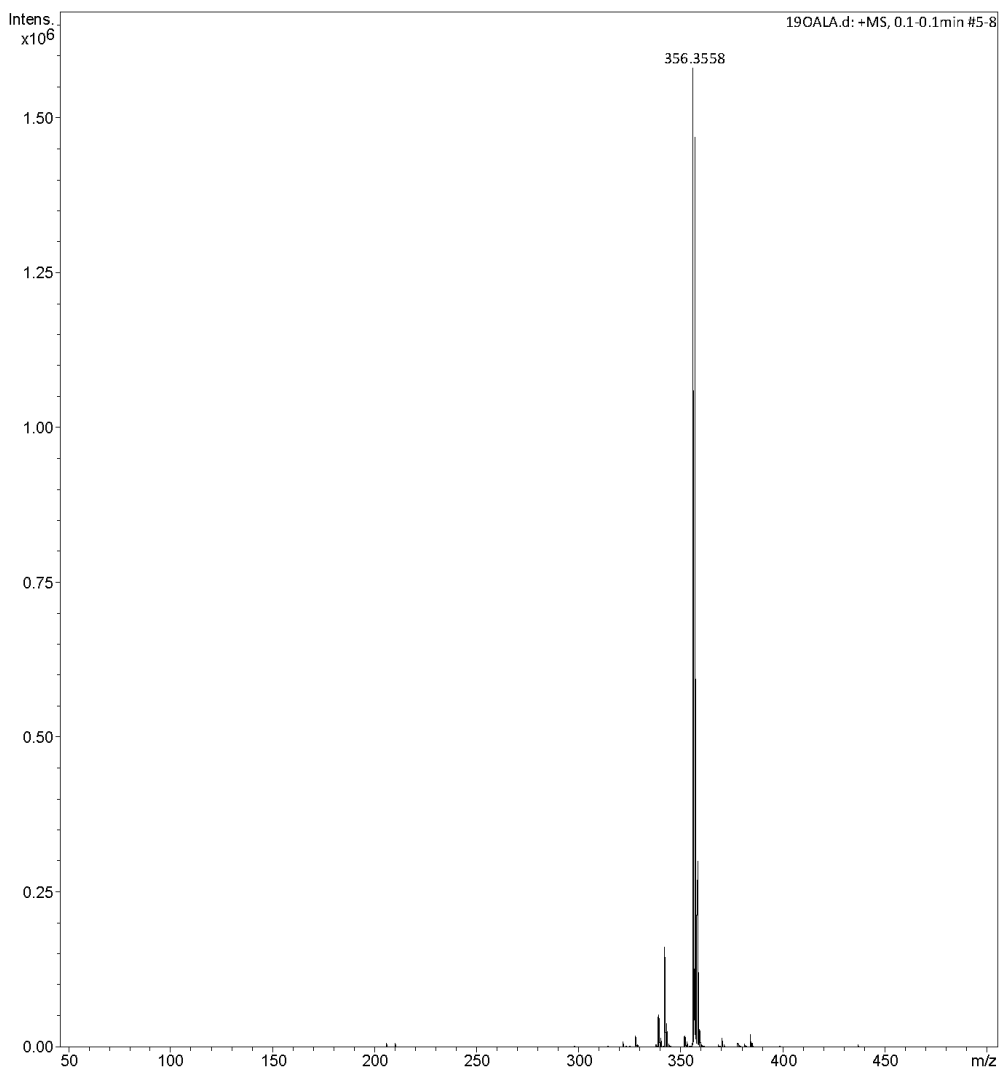


Figure S27. ESI mass spectrum of *O*-nonadecanoyl-L-alaninol.

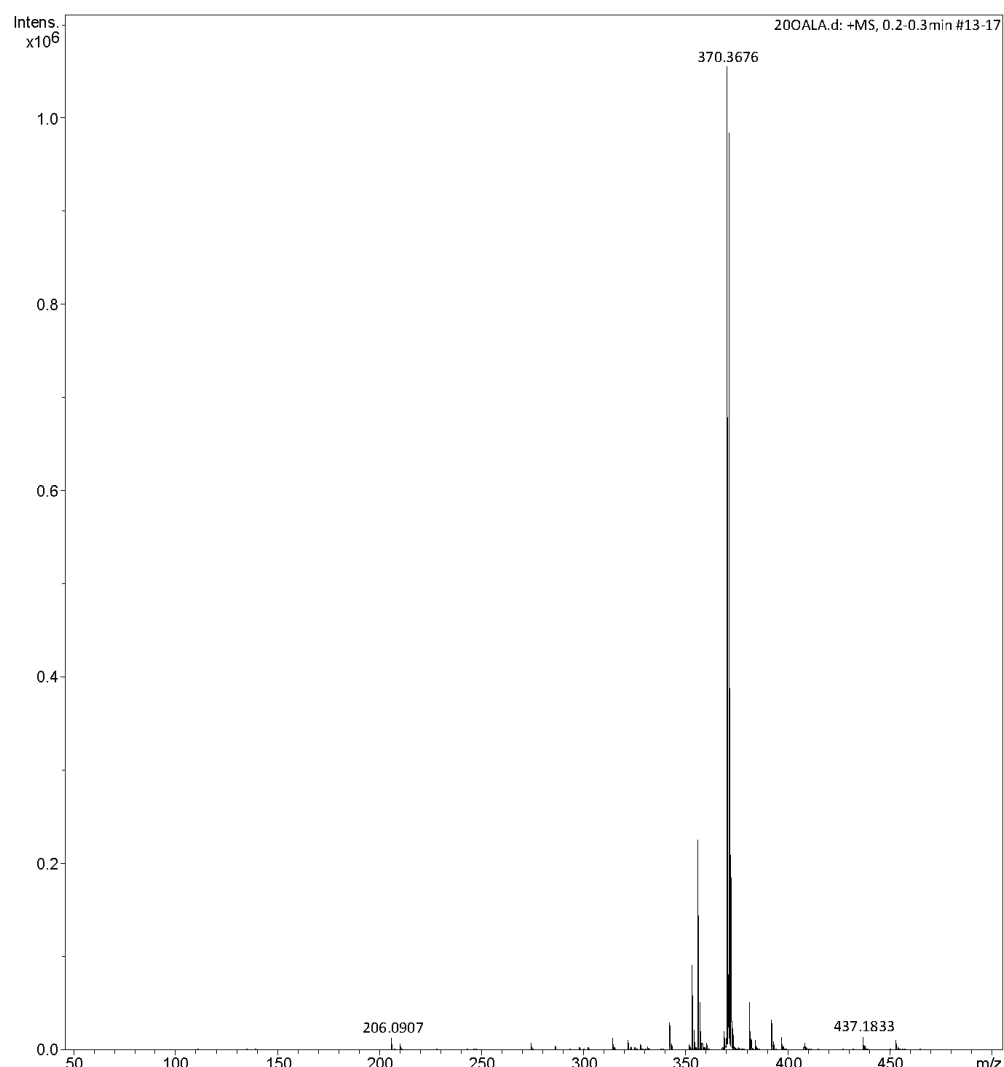


Figure S28. ESI mass spectrum of *O*-eicosanoyl-L-alaninol.

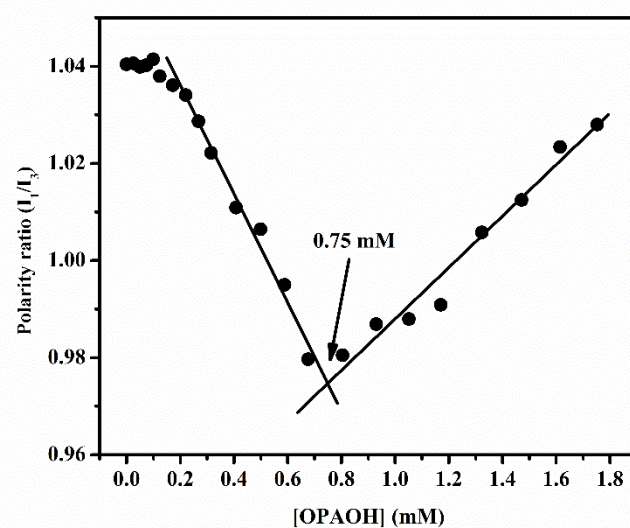


Figure S29. Determination of the CMC of *O*-palmitoyl-L-alaninol (OPAOH).

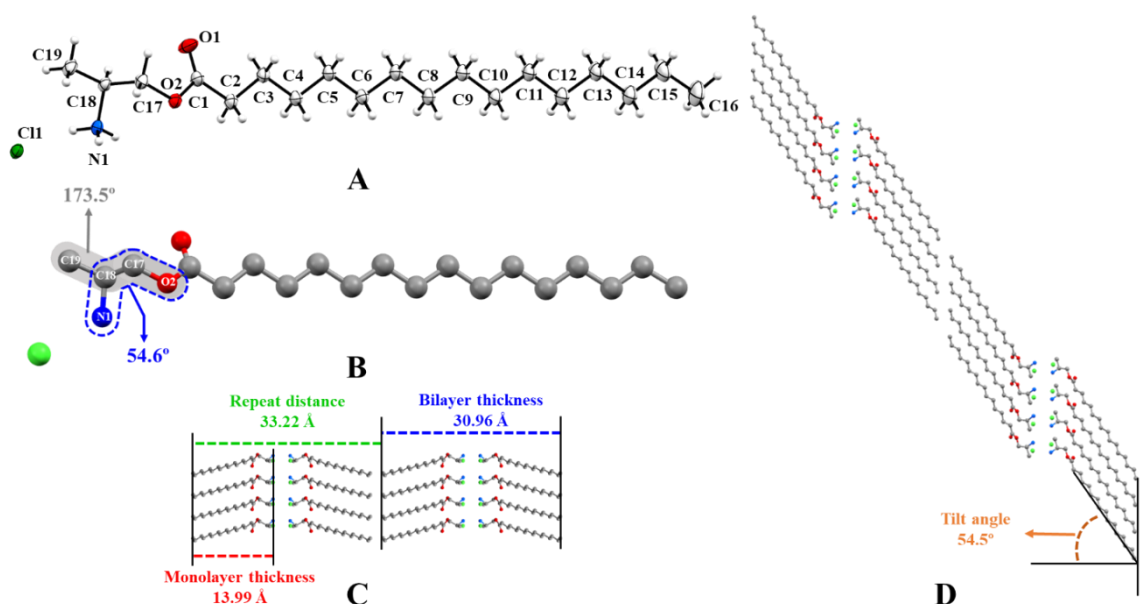


Figure S30. Molecular and crystal structure of *O*-pamitoyl-L-alaninol. **(A)** ORTEP of OPAOH. **(B)** Ball and stick representation of OPAOH structure highlighting two key torsion angles in the polar head group. **(C, D)** Packing diagrams viewed along the *a*-axis and *b*-axis, respectively. Hydrogens were omitted for clarity.

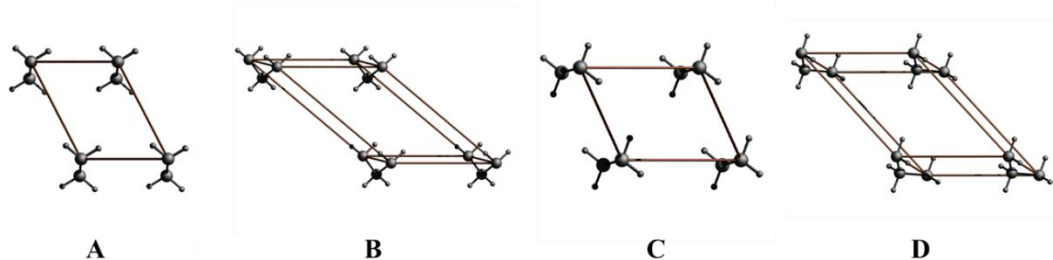


Figure S31. Subcell structure of OPAOH (**A**, **B**) and OHDAOH (**C**, **D**). Both subcells belong to the classic triclinic parallel ($T_{//}$) type.

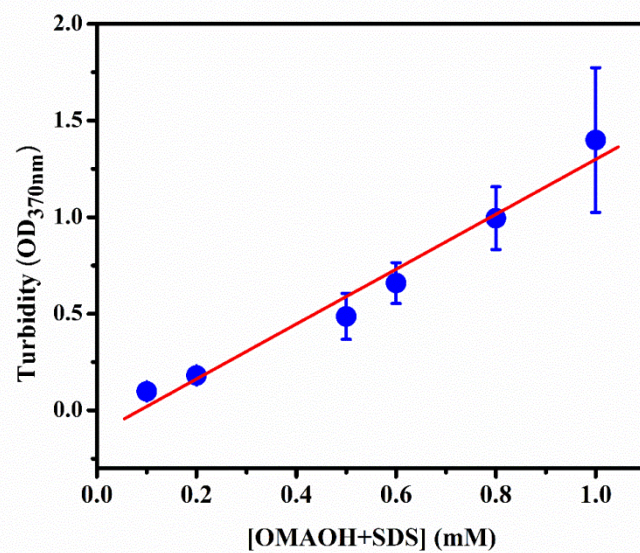


Figure S32. Effect of dilution on the turbidity of OMAOH-SDS catanionic liposomes. The cationic liposomes containing 0.5 mM each of OMAOH and SDS (total surfactant concentration = 1.0 mM) were diluted and the turbidity of the diluted samples was measured by monitoring optical density at 370 nm. Solid red line represents linear least squares fit.